NASA Technical Memorandum 101680

An Assessment of the Potential of Continuous-Wave Ranging for Measuring the Distance to a Highly Reflective, Infinite Sheet

C. P. Hearn
M. C. Bailey
M. J. Czerner
K. L. Dudley
E. Vedeler

April 1990

National Aeronautics and Space Administration

Langley Research Center
Hampton, Virginia 23665-5225

Summary

A stated objective of the Aft Flow Ionization Experiment (AFIE) is to measure the distance from a spacecraft antenna to a highly-ionized plasma surface in terms of the phase angle of the antenna reflection coefficient. The total system consists of the antenna and phase-measurement subsystems. This paper is primarily concerned with the antenna subsystem and the theoretical relationship between the phase of the reflection coefficient and the distance to a highly reflective boundary. It is concluded that radiation loss (energy coupled into the region between the antenna ground plane and the reflecting boundary, which is then radiated out the sides) distorts the phase-distance relationship that would exist in an idealized nonradiating system and, thereby, degrades the accuracy of the distance measurement. Radiation loss increases as aperture size decreases; therefore, small-aperture, large-beamwidth antennas are undesirable for this application. The theoretical conclusions of this paper are supported with laboratory measurements.

Background

The AFIE distance measurement approach is a direct outgrowth of the RAM project, described in [1]. This primary reference, the references cited therein, and some more recent works are used to assess the success potential of the AFIE. The RAM distance-measuring concept is based on the assumptions that (a) the electron density of the plasma is such that the plasma can be modeled as a perfectly reflecting flat surface with a reflection coefficient $\Gamma_\rho = -1$ and (b) the antenna, transmission media, and plasma can be collectively modeled as a shorted transmission line for which the reflection coefficient, Γ_s, can be expressed as

$$\Gamma_s = \frac{V_{reflected}}{V_{forward}} = \Gamma_\rho e^{-2\gamma d} \cong -1e^{-2\gamma d} \qquad (1)$$

where $\gamma = \alpha + j\beta$ is the complex propagation constant and d is the one-way path length. The phase of Γ_s, θ_s, is

$$\theta_s = \pi - 2\beta d = \pi - 4\pi(d/\lambda) \qquad (2)$$

as stated in [1], p. 14. Note that θ_s is independent of loss with this model, since nonzero values of α affect only the magnitude of Γ_s, ρ. Reference [2] is cited in [1] as providing theoretical justification for this model and validating the linear relationship between θ_s and d, given by (2). However, a thorough evaluation of [2] leads us to conclusions fundamentally different from those stated in [1], primarily because the circuit model developed in [2], p. 17, is considerably more complex than the simple shorted, lossy transmission line described by (1) and (2) and includes additional shunt elements to account for radiation loss and energy storage. The variance between these models becomes very pronounced when the aperture is much less than a wavelength and the near-field becomes more spherical. In the circuit analogy, radiation is modeled by adding shunt conductance, g, to the propagation-loss conductance associated with that portion of the transmitted signal which is reflected back into the antenna. Susceptance, b, is due to energy storage in nonpropagating evanescent modes at the aperture discontinuity or in the fields of the hypothetical transmission line between the aperture and the reflecting boundary. The total admittance, y, is the sum of the individual components and, therefore, produces a different reflection coefficient (and hence phase angle) than would a nonradiating system.

To illustrate the effects of radiation conductance, consider an idealized case in which all b is attributable to the hypothetical transmission line and all g is attributable to radiation loss. Without loss ($g = 0$), the locus of $\Gamma_s(d)$ is the perimeter of the Smith chart ($\rho = 1$), as shown in figure 1a, ($b = -1$), and θ_s is proportional to d, as given by (2). With loss, ($g > 0$), the locus of $\Gamma_s(g)$ for an arbitrary, but fixed, value of b is along the appropriate contour of constant b, as in figure 1b, ($g = 1$ and $b = -1$). $\theta_s(g)$ with $g = 1$ differs by about 27° from that with $g = 0$. In general, $\theta_s(g)$ changes with g in a nonlinear manner by an amount that can approach 180°! It is shown in figure 4 of [2] that g is a strong function of d and is zero when $d = n\lambda/2$ (because $\rho = 1$ and there is no loss), and b is maximum at these distances. Actually, the physical situation is not so simple as this example, and the susceptance of nonpropagating modes significantly affects θ_s, as will be shown.

Theoretical Results

The actual AFIE antenna is presently defined only to the extent of far-field performance specifications which will satisfy the communications requirements in the absence of plasma. This section considers how well the complex reflection coefficients of two theoretical models of radiating apertures having perfectly conducting sheets in the near-field can be used to measure distance to the reflecting plane. In addition to the infinite-slot model of [2], a more recent model of a circular waveguide exciting infinite parallel plates has become available [3] which has the flexibility to include a multilayer dielectric sheet over the aperture, as is the case with the AFIE. The effects of aperture size and the presence of a dielectric slab representative of Space Shuttle tile are considered, with phase error defined as the maximum deviation of θ_s from the straight line having a slope of $-4\pi(d/\lambda)$, as in (2), and an intercept corresponding to the phase at d = 0. Thus, the intercept is not restricted to π, as in (2). This amounts to an initial calibration in which the reflecting plate is located at d = 0, as advocated in [1].

The phase-measurement technique proposed for the AFIE requires the reflection-coefficient magnitude to be no less than 0.316, corresponding to a return loss of -10 dB or less, [1]. Thus, any value of d for which $\rho < 0.316$ is considered to be outside the usable range of the measurement. When plotted as a function of d, θ_s is roughly repetitive in $\lambda/2$ zones and ρ exhibits points at $\lambda/2$ intervals at which it approaches unity. Thus, the ambiguity associated with a phase measurement must be resolved in order to ascertain the correct $\lambda/2$ zone if measurements beyond $d = \lambda/2$ are required.

A major, though unproved, contention of [1] was that reducing the "free-space mismatch" of the antenna to zero (with a tuner) would guarantee linearity between θ_s and d. The linear transformation corresponding to free-space impedance matching is applied to the input admittances of both models and shown to have mixed effects on θ_s-d linearity.

I. Infinite-slot aperture [2].

The input admittance plots of [2] were transformed so that the antenna was impedance matched with d = oo. The variables ρ and θ_s were computed and plotted against d in figures 2 through 12 for normalized slot widths ($w = W/\lambda$) of 0.1, 0.278, 0.6 and 1.0, with and without free-space impedance matching. The "matched" curves were all initialized to 180° at d = 0 to facilitate interpretation. In all cases, the straight line described by (2) was included for comparison. The results are summarized in Table I where the maximum

distance-measurement error in each zone is tabulated for various parameters. It can be seen that:

(a) Radiation loss defeats the measurement over much of the w-d matrix, including the first zone for w = 0.1, as indicated by shading.

(b) "Phase capture" occurs beyond the first zone for w = 0.1 and 0.278 due to the large free-space mismatch. Phase capture occurs when the signal reflected from the sheet is smaller than the reflection from the aperture discontinuity, and the phase of the sum is dominated by the large signal.

(c) Matching eliminates phase-capture in the higher zones and reduces the phase error by about 24 percent in the first zone for w = 0.1 and 0.278. Matching increased phase error in all zones for w = 0.6; with w = 1.0, the aperture was essentially matched (see fig. 27).

(d) Increasing w is always helpful because the radiated energy is more collimated and less is lost to radiation into the parallel-plate waveguides.

(e) ρ generally (but not always, see fig. 7) decreases as d/λ increases and additional propagating modes are introduced. Thus, only the first zone ($d/\lambda < 0.5$) is usable unless $w \geq 0.6$.

II. Circular waveguide aperture [3].

The physical model for this case is shown in figure 13. A circular waveguide aperture having a normalized dimension of A = Diameter/λ radiates into infinite parallel ground planes. The medium between the ground planes is assumed to have a complex relative permittivity of (1.0-j0.00001). Plots of θ_s and ρ versus d are shown in figures 14 through 17 and the results are summarized in Table II. More detail on the variation of θ_s from the straight line defined by (2) is given by figures 18 and 19. Matching is beneficial only for A = 0.6, where the phase error in the first zone is reduced by about 40 percent and the "phase-capture" effect evident in figure 14 is eliminated. Matching has little effect for A > 0.6. It can be seen from (2) that the distance-measurement error in wavelengths is found by dividing the phase error, in radians, by -4π (or if the phase error is in degrees, by

-720). Another major observation is that only when $A \geq 1.5$ and $\rho > 0.316$ can a measurement be made beyond $d = \lambda/2$.

III. Circular waveguide covered with dielectric sheet [3].

As shown in figure 20, a multilayer dielectric sheet representative of Space Shuttle tile covers the aperture. Plots of θ_s and ρ are shown in figures 21 through 24, with the results summarized in Table III. The deviation of θ_s from (2) is plotted in Figures 25 and 26. Matching is, as before, primarily beneficial in reducing phase capture but does not otherwise significantly improve θ_s-d linearity. The dielectric sheet causes additional radiation loss due to surface-wave propagation, and the total loss is so great that for $A = 0.6$ and 0.8, ρ is too small, even in the first zone, to measure phase. When $A \geq 1.5$, the free-space match improves greatly, there is no evidence of phase-capture, and ρ is sufficient to make a measurement, if the resulting linearity is acceptable; the case $A = 3$ allows measurements out to at least two wavelengths.

To the extent that this model is a reasonably accurate representation of the AFIE antenna, the results are ominous because they show that a fundamental conflict exists between the aperture size requirements for distance-measurement and communications purposes.

The effect of aperture size on the free-space voltage standing-wave ratio (VSWR) of the three models is shown in figure 27. The infinite slot cutoff is at $w = 0$, whereas the circular aperture cutoff is at $A = 0.586$. It can be seen that $w \geq 0.6$ for the infinite slot and $A \geq 0.8$ for the circular aperture without tile will keep the VSWR below 1.2:1. With tile present, matching will lower the residual VSWR of the larger apertures, which is seen in Table III, to slightly improve the linearity by reducing internal reflections.

IV. Application to Reference 1.

It is of interest to examine [1] for results which pertain to the conclusions of this paper. The model of figure 20 is applied to the S-band (3.348 GHz) antenna of [1], for which some measured results are available. The antenna in [1] differed slightly from the theoretical model of [3], which is more appropriate for the AFIE, in that it was only partially loaded with a dielectric plug. The behavior of this antenna as predicted by [3] is compared in figure 29 with measured data from [1], where it is seen that only the first zone is usable. Figures 28 and 30 show that the maximum phase error in the first zone is about

55°. The slight deviation of figure 29 from figure 8(b) of [1] is possibly due to the finite size or lack of parallelism of the reflecting plates.

It is also noteworthy that the L-band antenna in [1] was unusable for phase measurement even in the first zone. Only at X-band where the physical aperture was 1.69λ could a phase measurement be made beyond 5 cm, because $\rho < 0.316$.

Additional Accuracy Considerations

In addition to the theoretical issue of nonlinearity between θ_s and d, the primary focus of this paper, there are a number of other factors that can further degrade the distance-measurement accuracy. This section briefly discusses a number of these factors that have been identified.

I. Four-probe phase-measurement technique.

The four-probe phase-measurement technique is crude by modern standards and useful only when the return loss is less than - 10 dB ($\rho = 0.316$), as noted earlier. This is because the ratio of maximum-to-minimum voltage from a square-law detector monitoring the E-field along a transmission line decreases with ρ, as shown below:

return-loss, dB	ρ	ρ^2	$(V_{max}/V_{min})^2$
0	1	1	oo
-3	0.707	0.5	33.94
-10	0.316	0.1	3.70
-20	0.1	0.01	1.49

According to [1], the additional phase error caused by a -10 dB return loss ($\rho = 0.316$ and 90 percent of the incident power is radiated or lost through dissipation) is on the order of 10 electrical degrees. The results presented here demonstrate that phase errors greatly exceeding 10° can occur with values of ρ much greater than 0.316, for example, the first zone in figures 16 and 18.

An additional difficulty associated with this phase-measurement technique is the ambiguity which arises when the net path length beyond the calibration plane exceeds $\lambda/2$. In principle, one might use the variation of ρ with d, $\rho(d)$, to resolve the ambiguity, but it can be seen from the $\rho(d)$ plots that this approach is highly questionable beyond the first zone because the difference between values of ρ corresponding to additional $\lambda/2$ increments is quite small.

II. Plasma assumptions.

The fact that the reflecting boundary is an imprecisely-characterized plasma instead of a perfectly conducting sheet raises a number of questions and concerns. For example,

(a) there is no theoretical assurance that the effective plasma reflection coefficient in (1) is π for finite apertures; a preflight calibration with a shorting plate cannot resolve this uncertainty,

(b) the boundary between free space and the plasma medium is not abrupt, but gradual, producing a net reflected wave that is the vector sum of many individual reflections occurring over a finite distance,

(c) geometrical variations from the theoretical models (specifically, the plasma is not perfectly flat, but will have some curvature) and lack of parallelism between the conducting surfaces of the spacecraft and the plasma (tilt) may cause further reduction in the returned signal level, and

(d) change of path propagation velocity due to the presence of the plasma effects the wavelength in the medium, and hence, the inversion algorithm, (2).

III. The AFIE antenna.

Interfacing unobtrusively with a communications system which is being designed strictly from a communications viewpoint creates another layer of potential problems. For example,

(a) the transmitted signal is not continuous wave, but binary phase shift-keyed and occupies a bandwidth of about 6 MHz. This will tend to "blur" the phase measurement, particularly at the maximum values of d where phase dispersion is maximum,

(b) the source VSWR at the generator port of the probe network must be kept quite low to prevent significant source-mismatch reflections which produce the same type of phase-measurement errors as free-space mismatch,

(c) the fact that multiple antennas are used on a switched basis to assure full spatial coverage can be expected to complicate calibration and data processing,

(d) the multilayer, dielectric, nonablating heat shield profoundly affects the antenna characteristics, as was demonstrated here. Either something must be done to significantly reduce surface wave excitation and propagation, or a larger aperture used if there is to be any chance of a measurement, and

(e) preflight matching of the antenna will probably be incorrect for actual flight conditions because of the environmental dissimilarities, leading to a residual mismatch under actual flight conditions and associated phase error.

Experimental Results

A microstrip disk antenna was mounted on a 4 ft x 4 ft ground plane (9.35λ at 2.30 GHz) and the complex reflection coefficient measured with a vector network analyzer as a parallel reflecting sheet was moved out to distances up to 3λ. These data are plotted in figures 31 and 32 and are generally consistent with the predicted behavior. Phase capture is evident past the first zone although the measured "free space" return loss of the antennas was -27 dB. The measured maximum return loss in the first zone was -8.54 dB, corresponding to a ρ of 0.374. That the measured minimum ρ in the higher zones was no less than 0.55 was attributed to the fact that the measurements were made in a shielded room instead of an anechoic chamber. The maximum phase deviation of the measured data from (2) was about 48° in the first zone, a distance measurement error of about 0.067λ. These results are reasonably close to those for the matched slot-aperture configuration with $w = 0.278$, as can be seen in figure 7 and Table I.

Concluding Remarks

All of these issues, and perhaps more which now remain unidentified, must be addressed and quantified in order to arrive at an overall estimate of the usefulness of this distance-measurement technique; however, the following conclusions can be reasonably drawn on the basis of what is now known and was presented here:

(a) Due to the wide antenna beamwidth(s) mandated by the communications requirements and the corresponding loss of returned signal strength due to radiation, which is exacerbated by the nonablating heat shield, it appears highly unlikely that a distance measurement can be made with this technique even in the first zone ($0 < d < \lambda/2$) unless some method of reducing surface-wave excitation and propagation can be devised. In [1], the horns were deliberately extended through the dielectric to achieve this result.

(b) Resolution of phase ambiguity, which occurs when $d > \lambda/2$, with measured reflection coefficient magnitude data appears highly infeasible.

(c) Even in the $d < \lambda/2$ region, the nonlinearity between θ_s and d is quite significant with small apertures and may in itself be unacceptable, even in the complete, though unlikely, absence of other sources of error.

Based on the factors and considerations discussed here, it must be concluded that the AFIE distance-measuring scheme as now proposed appears to have a low probability of success. A final assessment can be made when a candidate AFIE antenna is available for testing in conjunction with actual, or closely simulated, nonablating tiles, which were shown here to have a significant impact on antenna performance in this application.

References

1. Grantham, W. L.: Flight Results of a 25000 foot-per-second Reentry Experiment Using Microwave Reflectometers to Measure Plasma Electron Density and Standoff Distance. NASA TN D-6062, December 1970.

2. Jones, J. E.; and Swift, C. T.: The Aperture Admittance of a Ground-Plane Mounted Waveguide Illuminating a Perfectly Conducting Sheet. NASA TN D-4366, March 1968.

3. Bailey, M. C.: CWG - A Fortran Program for Mutual Coupling in a Planar Array of Circular Waveguide-fed Apertures. NASA TM-101614, June 1989.

TABLE I.

Distance - measurement error for infinite slot aperture

Aperture Size (wavelengths)	Round-trip error in wavelengths, over:						
	0 to λ/2		λ/2 to λ		λ to 3λ/2		
	unmatched	matched	unmatched	matched	unmatched	matched	
0.1	0.17	0.13	phase capture	0.135	---	---	
0.278	0.065	0.05	phase capture	0.08	phase capture	0.085	
0.6	0.04	0.075	0.06	0.1	0.07	---	
1.0	0.03	0.03	0.05	0.05	0.07	---	

Denotes return loss > 10 dB , ($\rho < 0.316$)

TABLE II.

Distance - measurement error for circular aperture without tile

Aperture Size (wavelengths)	Round-trip error in wavelengths, over:							
	0 to λ/2		λ/2 to λ		λ to 3λ/2		3λ/2 to 2λ	
	unmatched	matched	unmatched	matched	unmatched	matched	unmatched	matched
0.6	0.197	0.121	phase capture	0.151	phase capture	0.161	phase capture	0.164
0.8	0.097	0.097	0.139	0.138	0.153	0.149	0.171	0.156
1.5	0.031	0.033	0.067	0.079	0.094	0.108	0.113	0.124
3.0	0.014	0.017	0.024	0.026	0.038	0.042	0.044	0.047

Denotes return loss > 10 dB , ($\rho < 0.316$)

TABLE III.

Distance - measurement error for circular aperture with tile

Aperture Size (wavelengths)	Round-trip error in wavelengths, over:							
	0 to λ/2		λ/2 to λ		λ to 3λ/2		3λ/2 to 2λ	
	unmatched	matched	unmatched	matched	unmatched	matched	unmatched	matched
0.6	0.176	0.057	phase capture	0.056	phase capture	0.067	phase capture	0.069
0.8	0.079	0.021	0.079	0.063	0.136	0.072	phase capture	0.099
1.5	0.054	0.046	0.083	0.067	0.099	0.076	0.107	0.099
3.0	0.019	0.014	0.028	0.025	0.039	0.031	0.054	0.047

Denotes return loss > 10 dB , ($\rho < 0.316$)

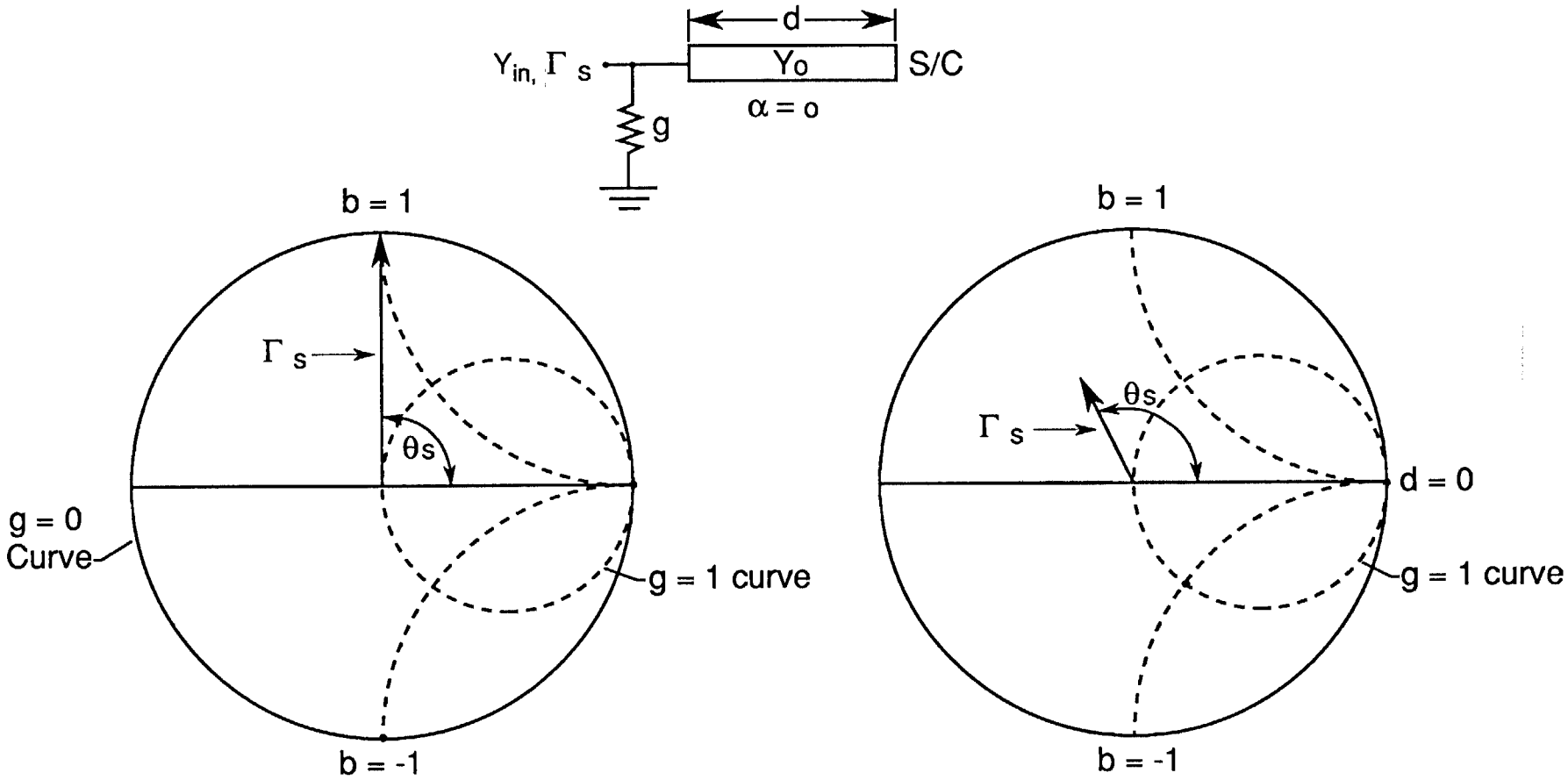

1a: g = 0, b = -1, θ_s = 90°

1b: g = 1, b = -1, θ_s = 117°

Figure 1.-Smith-chart representation of complex reflection coefficient (admittance co-ordinates)

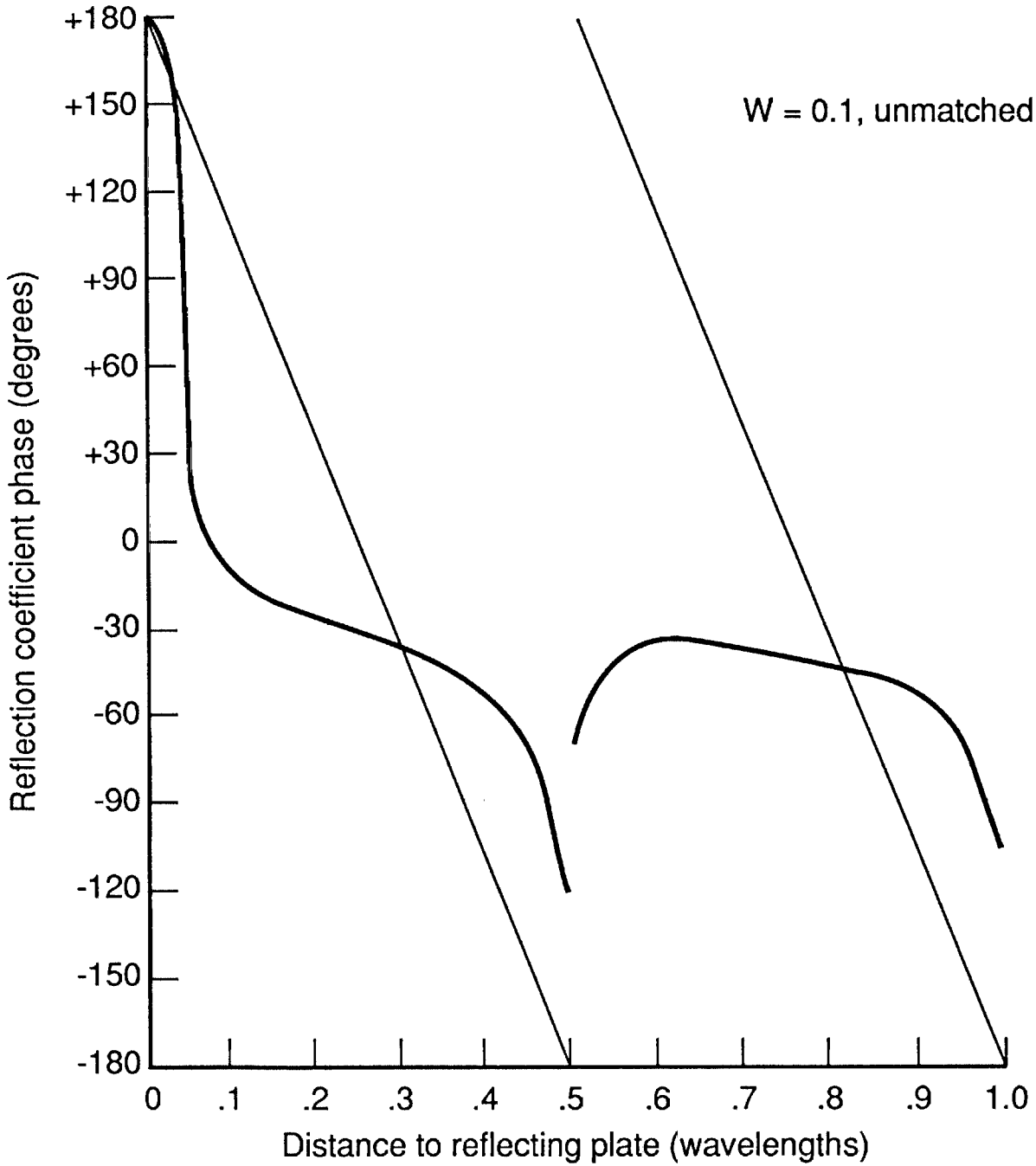

Figure 2.-Reflection coefficient phase vs. plate space.

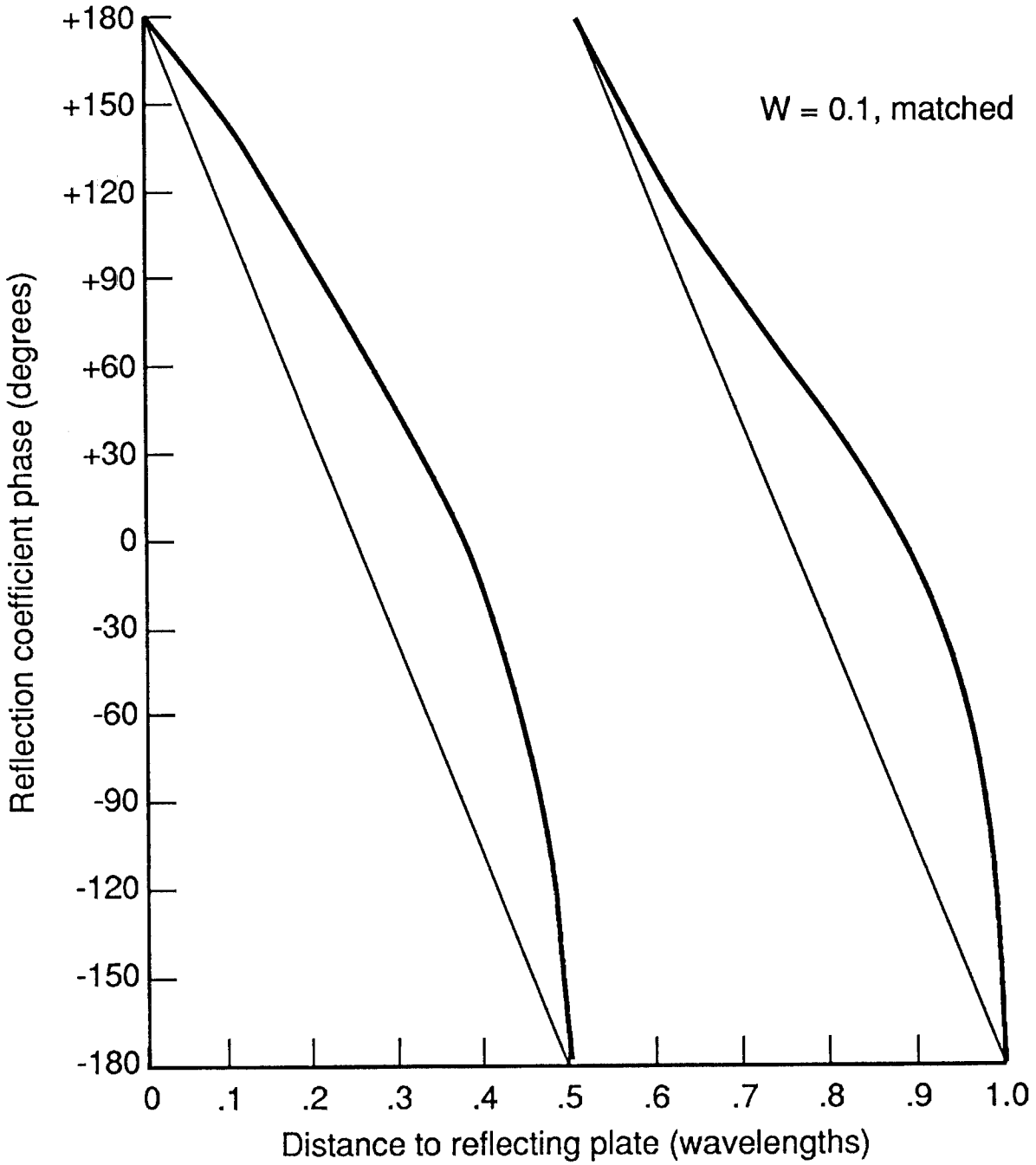

Figure 3.-Reflection coefficient phase vs. plate spacing.

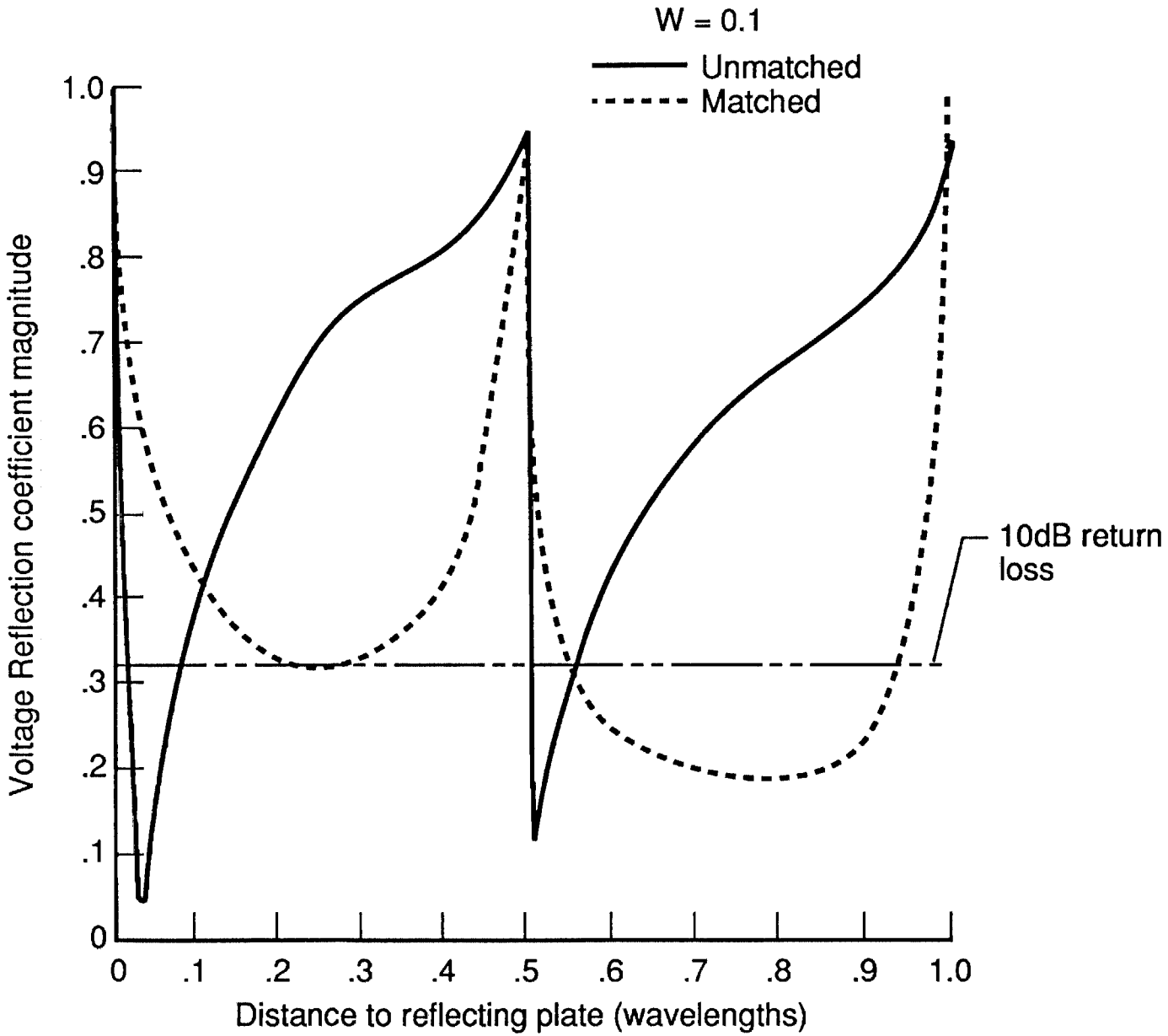

Figure 4.-Reflection coefficient magnitude vs. plate spacing.

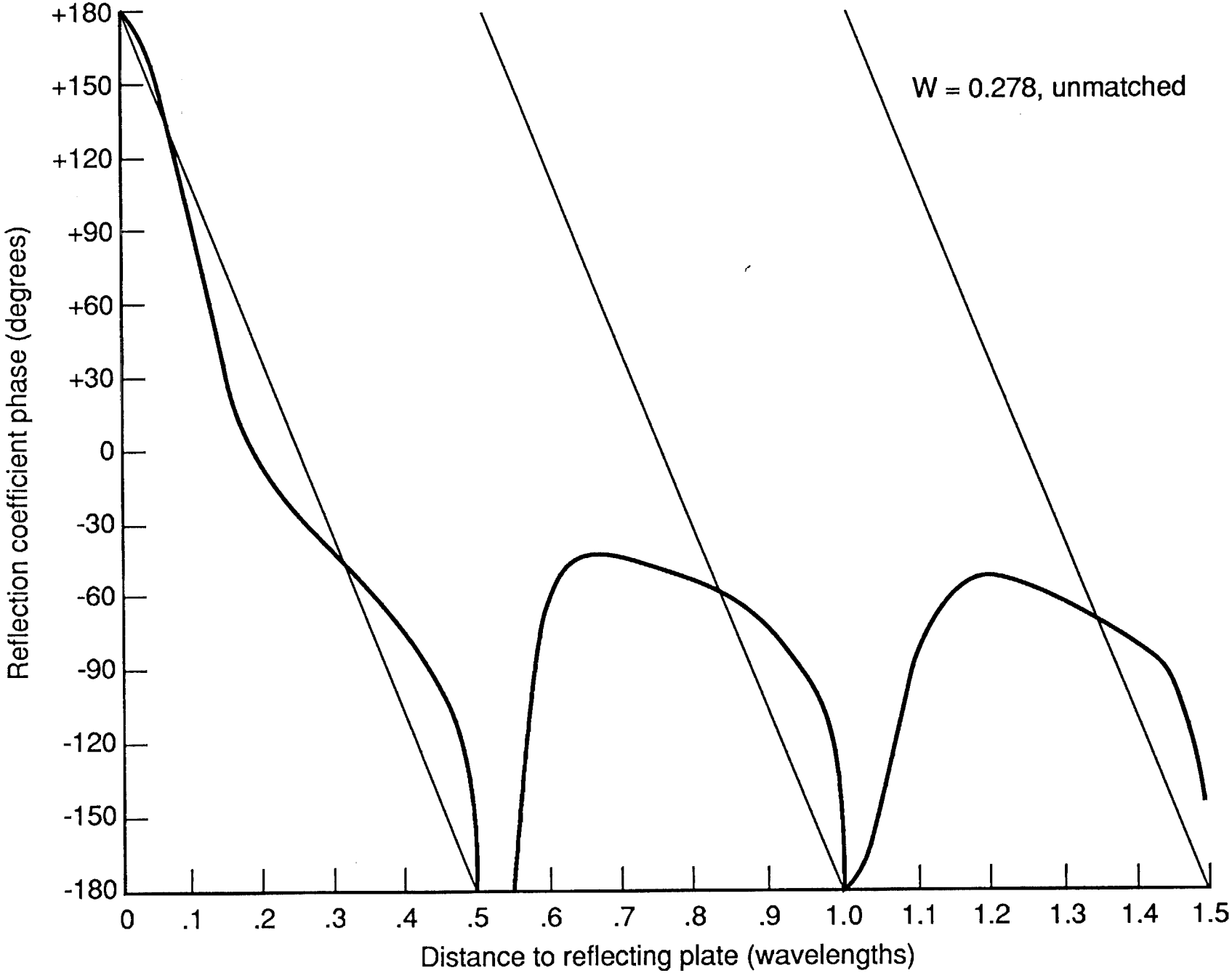

Figure 5.-Reflection coefficient phase vs. plate spacing.

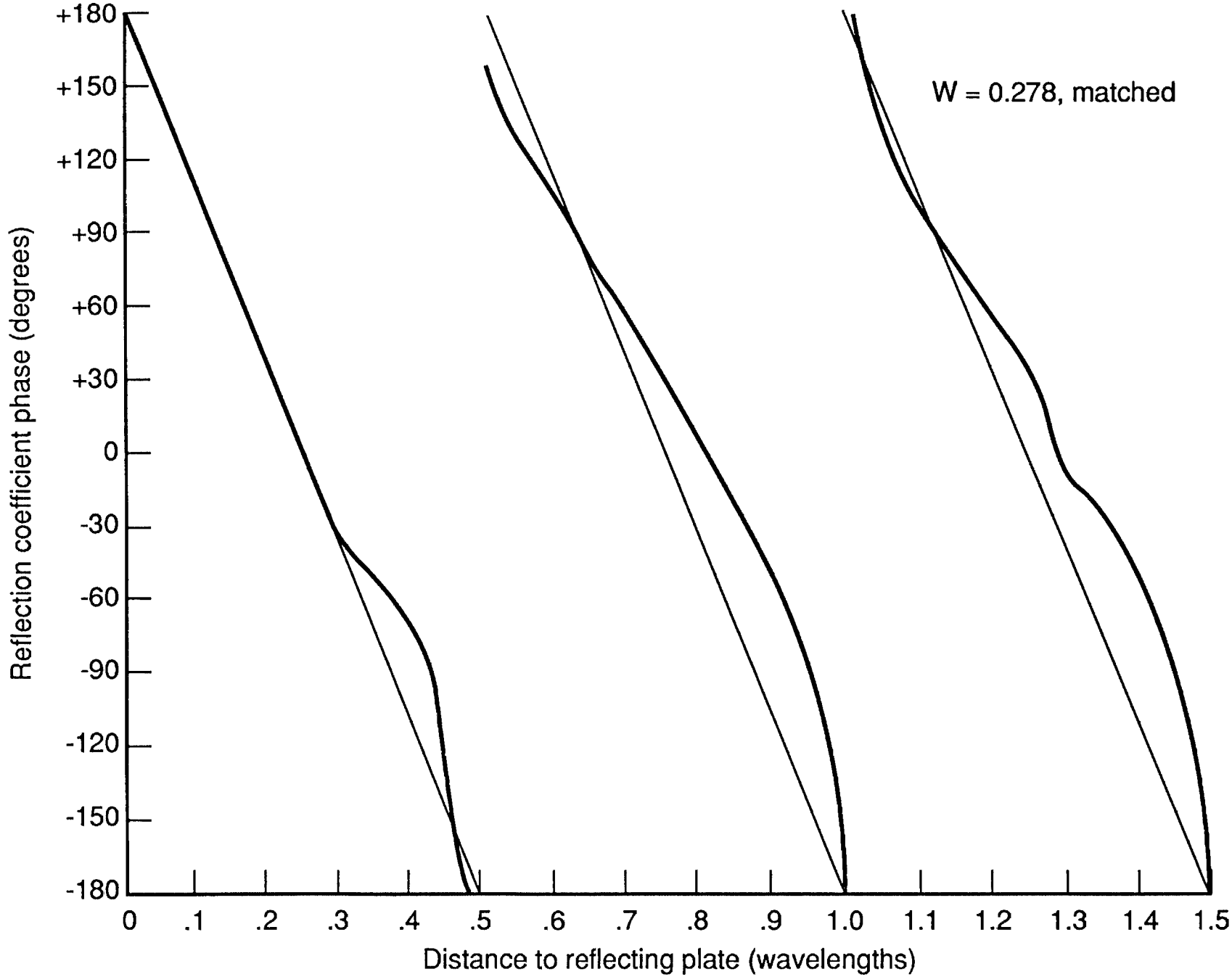

Figure 6.-Reflection coefficient phase vs. plate spacing.

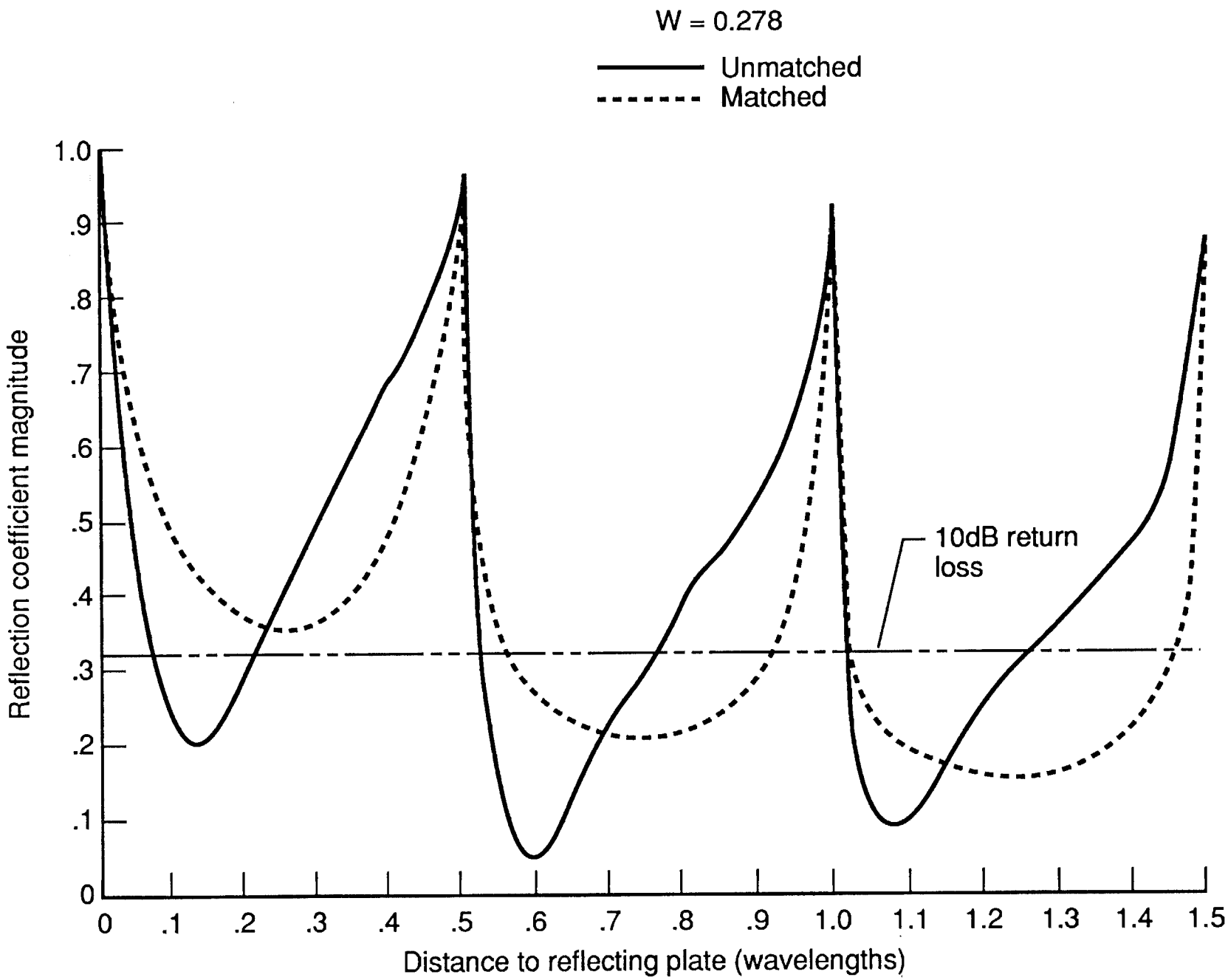

Figure 7.-Reflection coefficient magnitude vs. plate spacing.

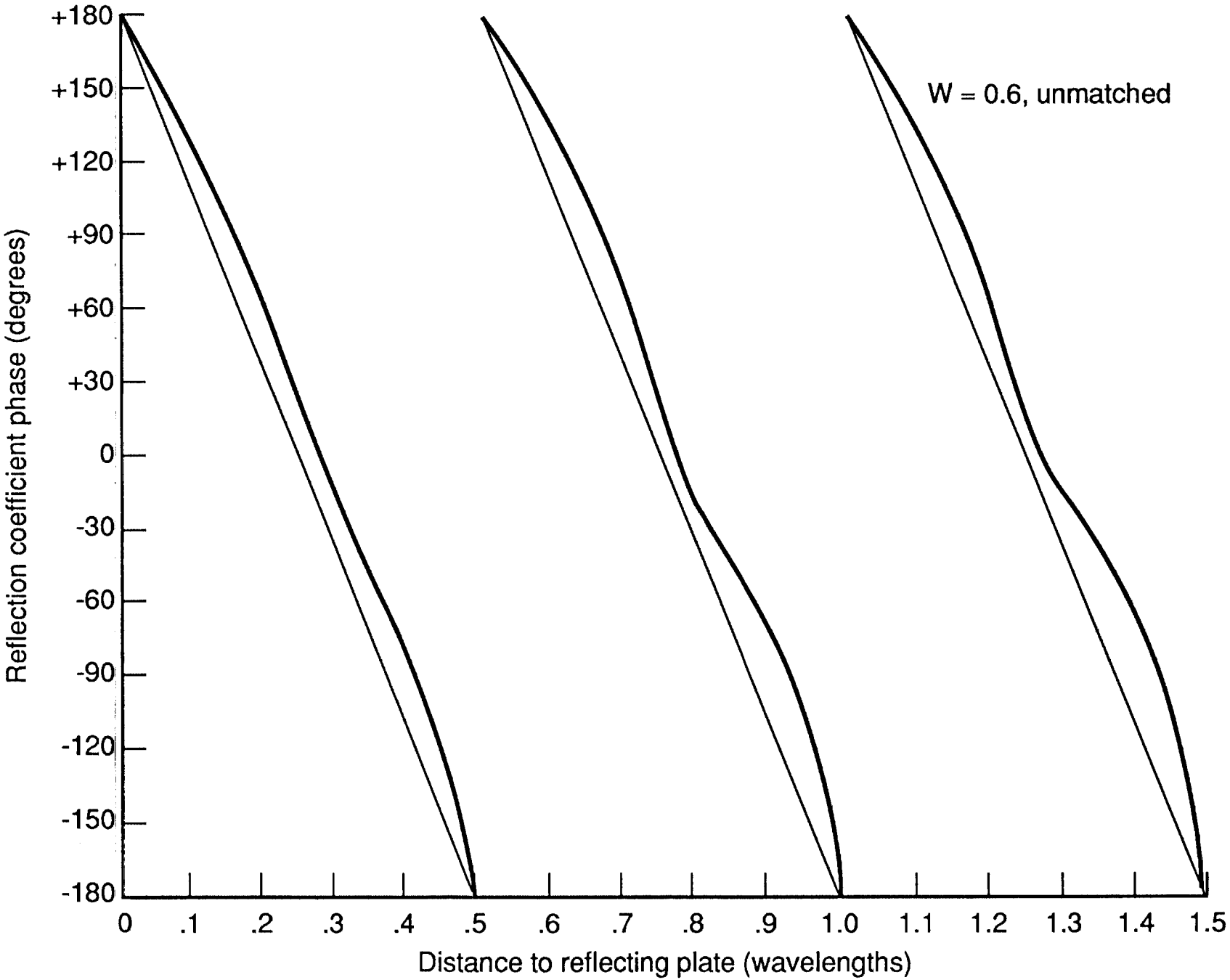

Figure 8.-Reflection coefficient phase vs. plate spacing.

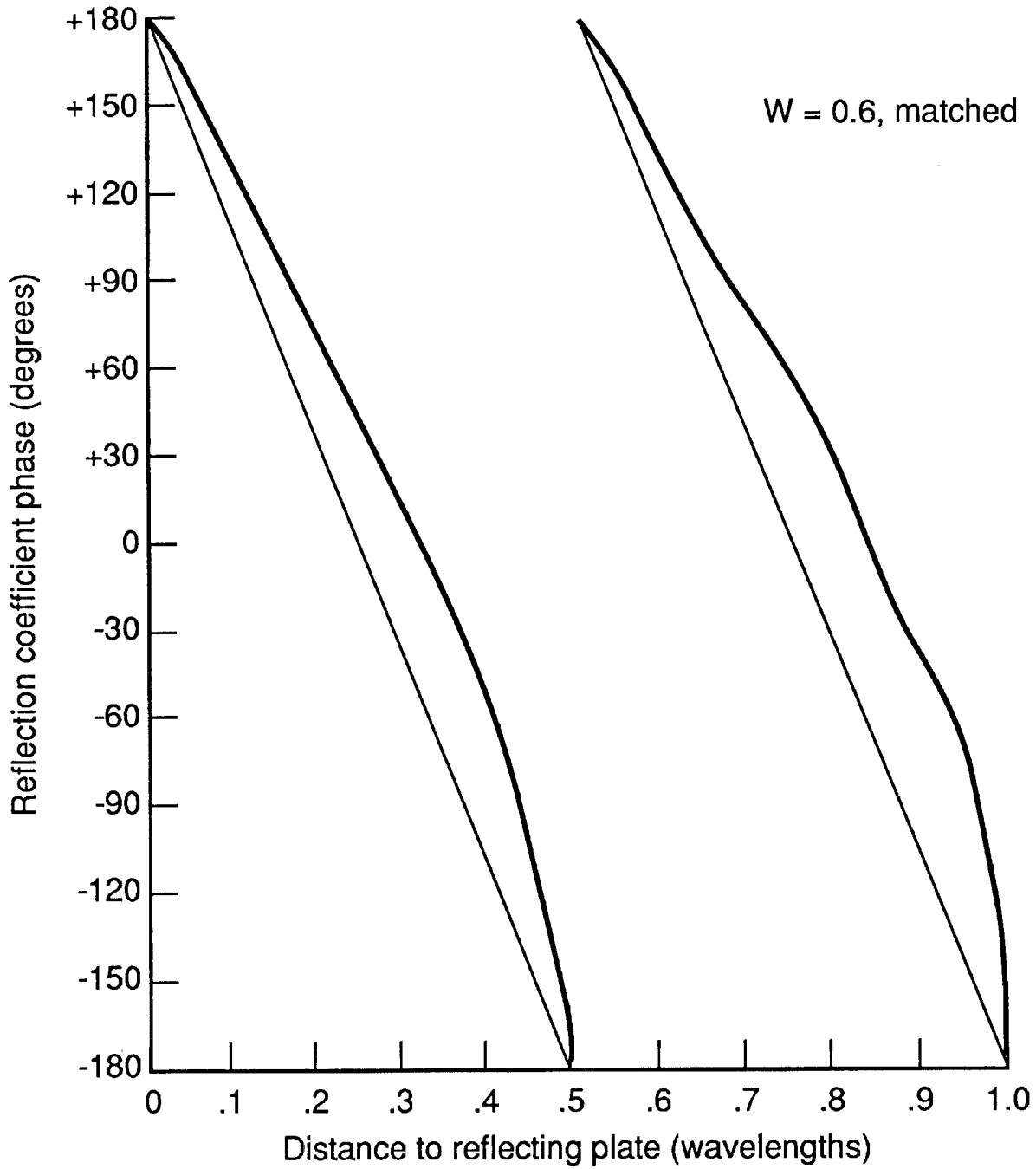

Figure 9.-Reflection coefficient phase vs. plate spacing.

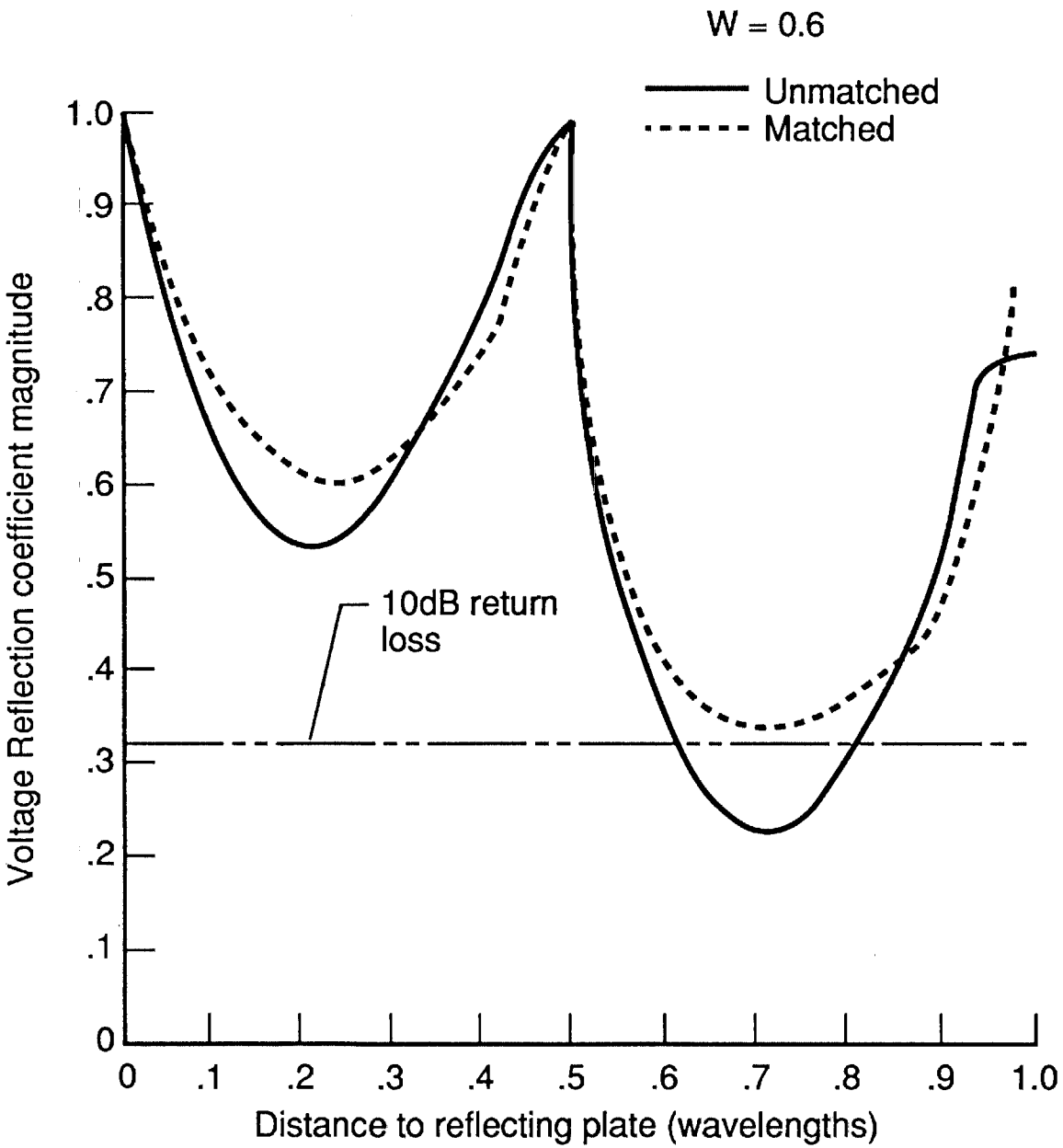

Figure 10.-Reflection coefficient magnitude vs. plate spacing.

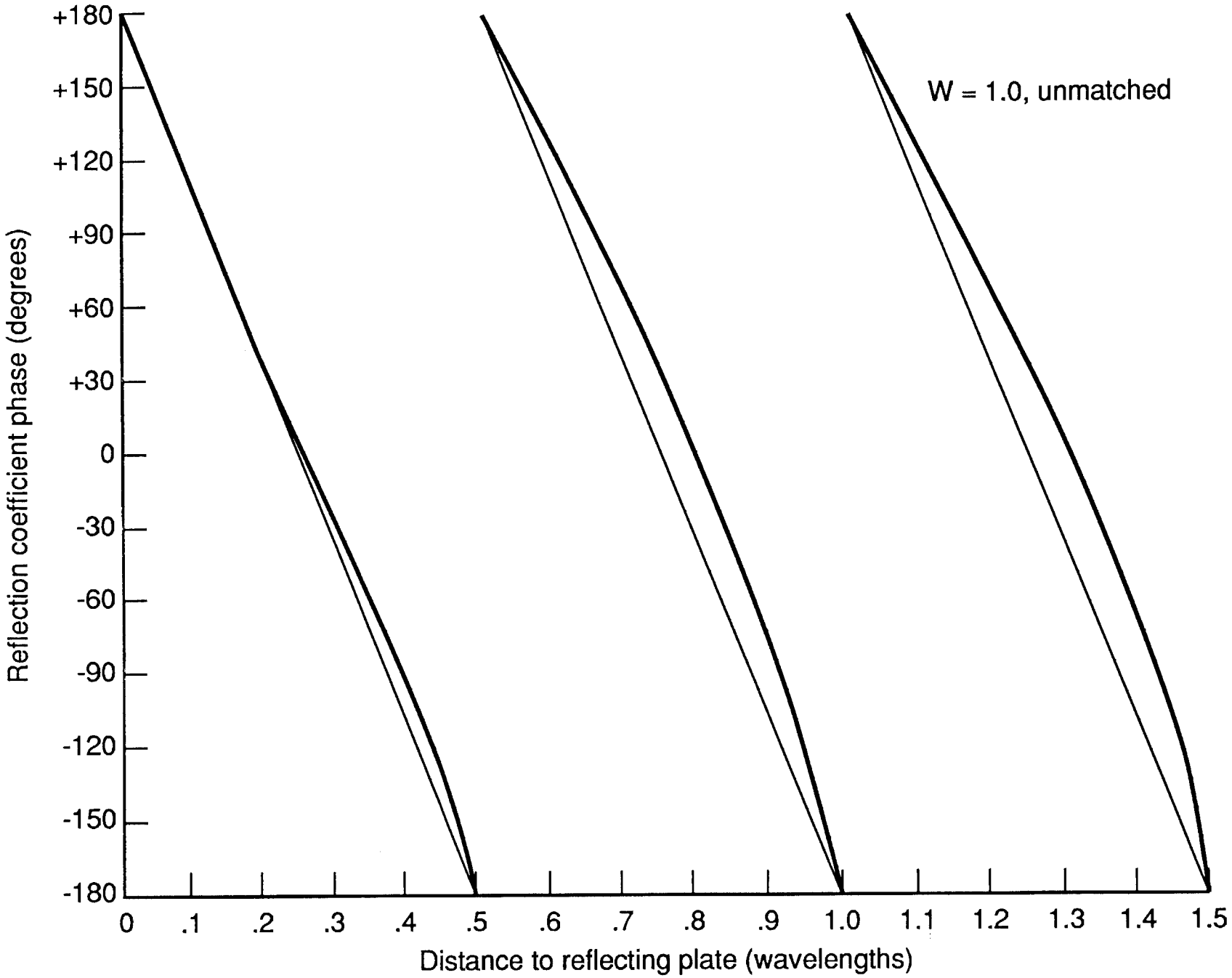

Figure 11.-Reflection coefficient phase vs. plate spacing.

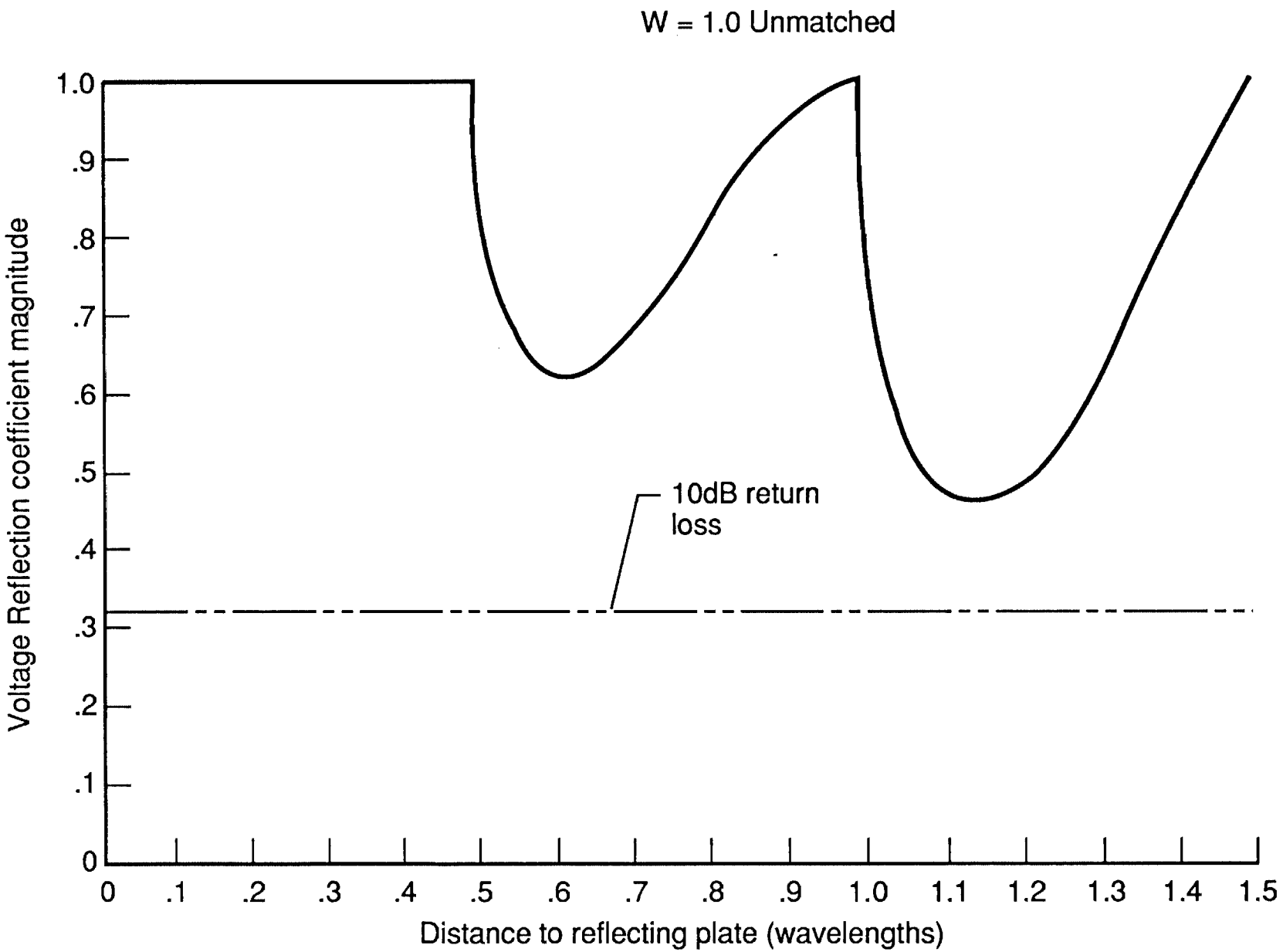

Figure 12.-Reflection coefficient magnitude vs. plate spacing.

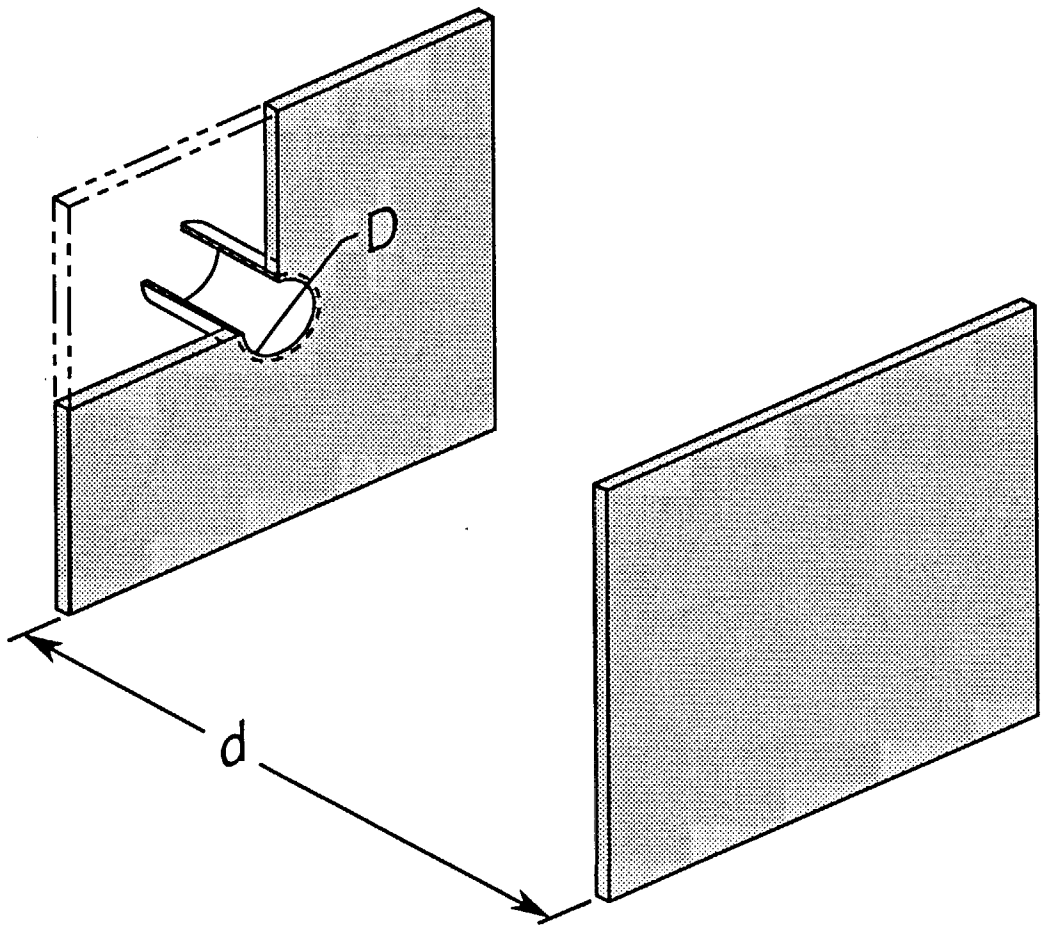

Figure 13.-Physical model of circular aperture and infinite reflecting plates.

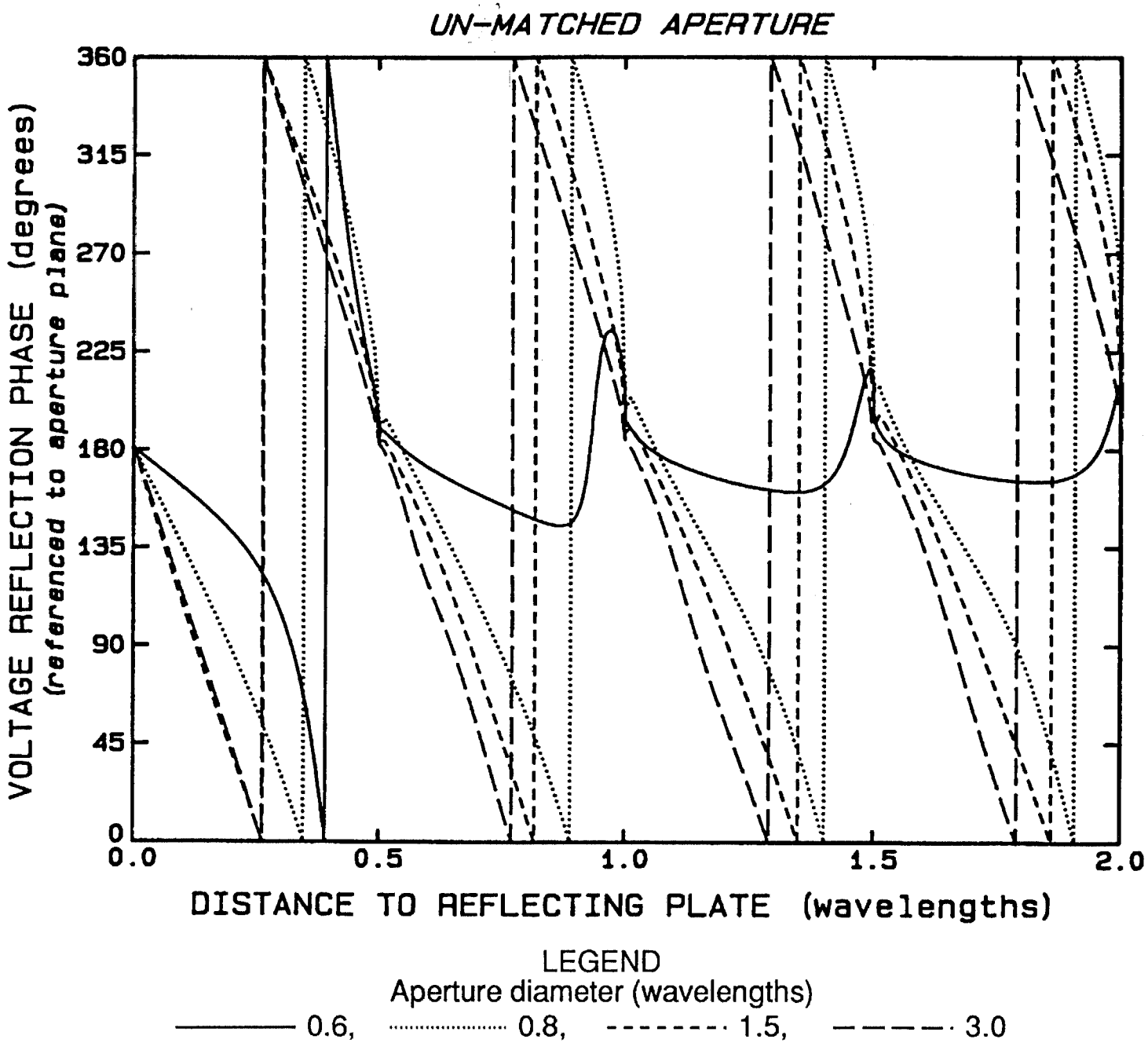

Figure 14.-Reflection coefficient phase vs. plate spacing.

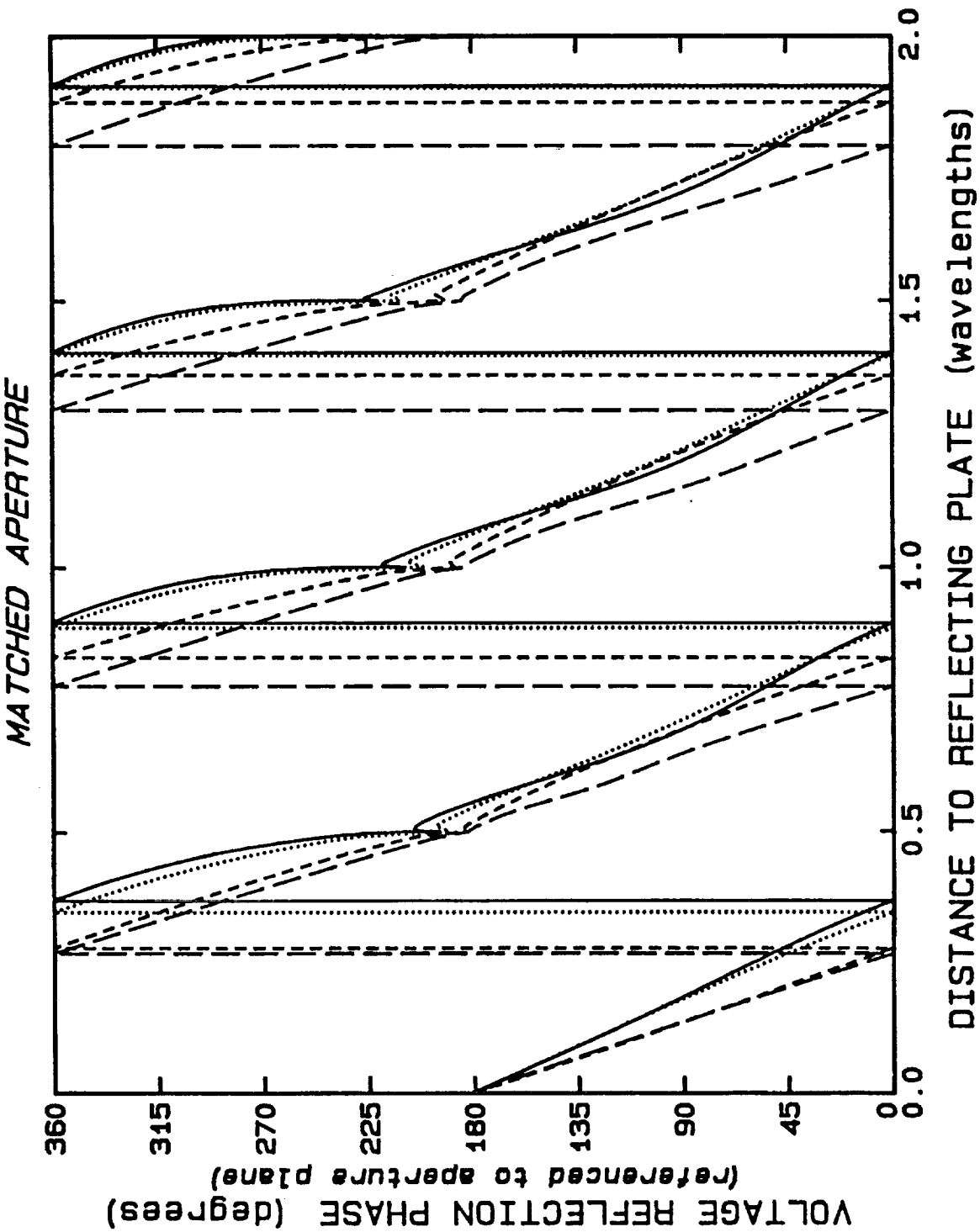

Figure 15.-Reflection coefficient phase vs. plate spacing.

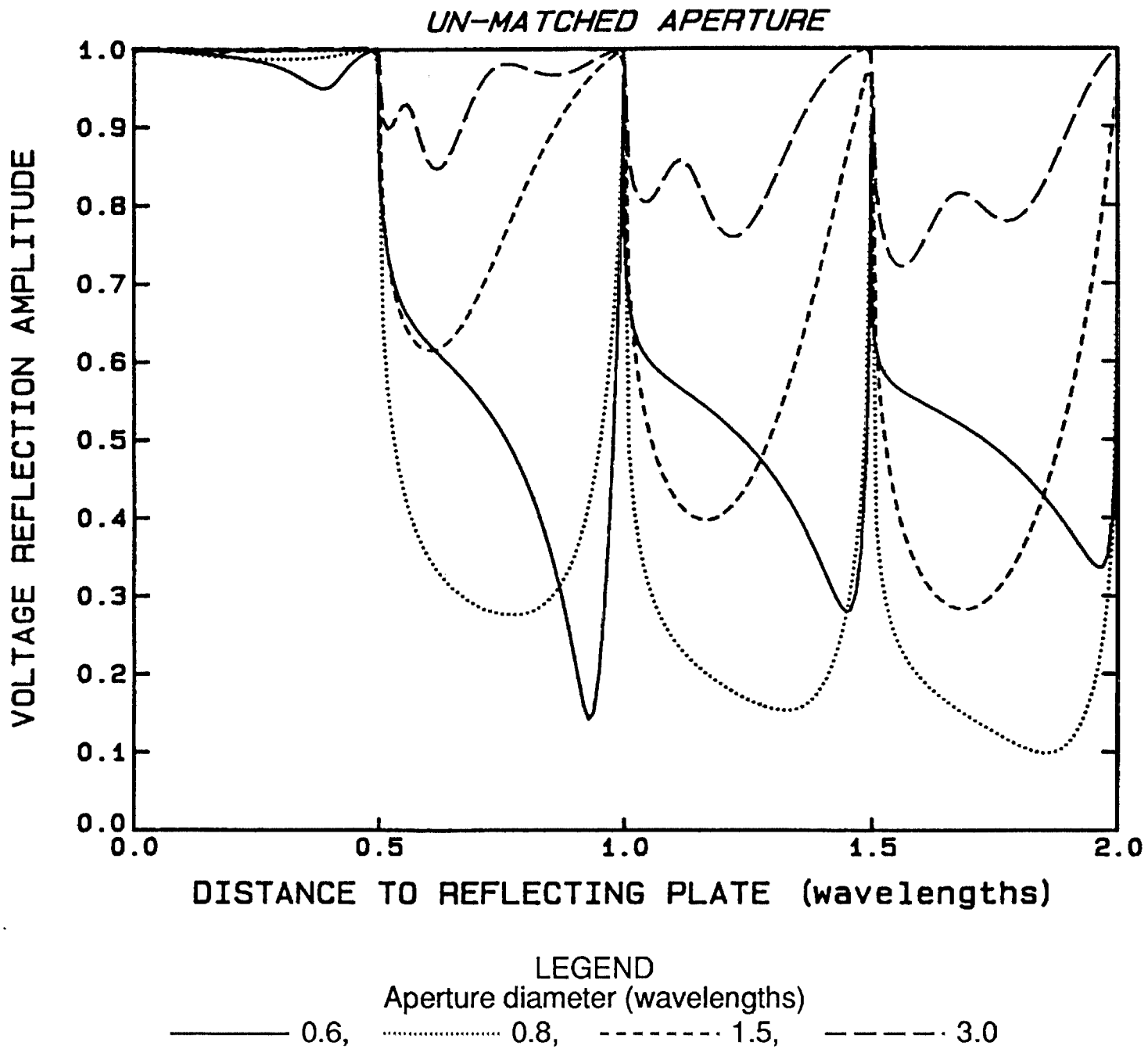

Figure 16.-Reflection coefficient magnitude vs. plate spacing.

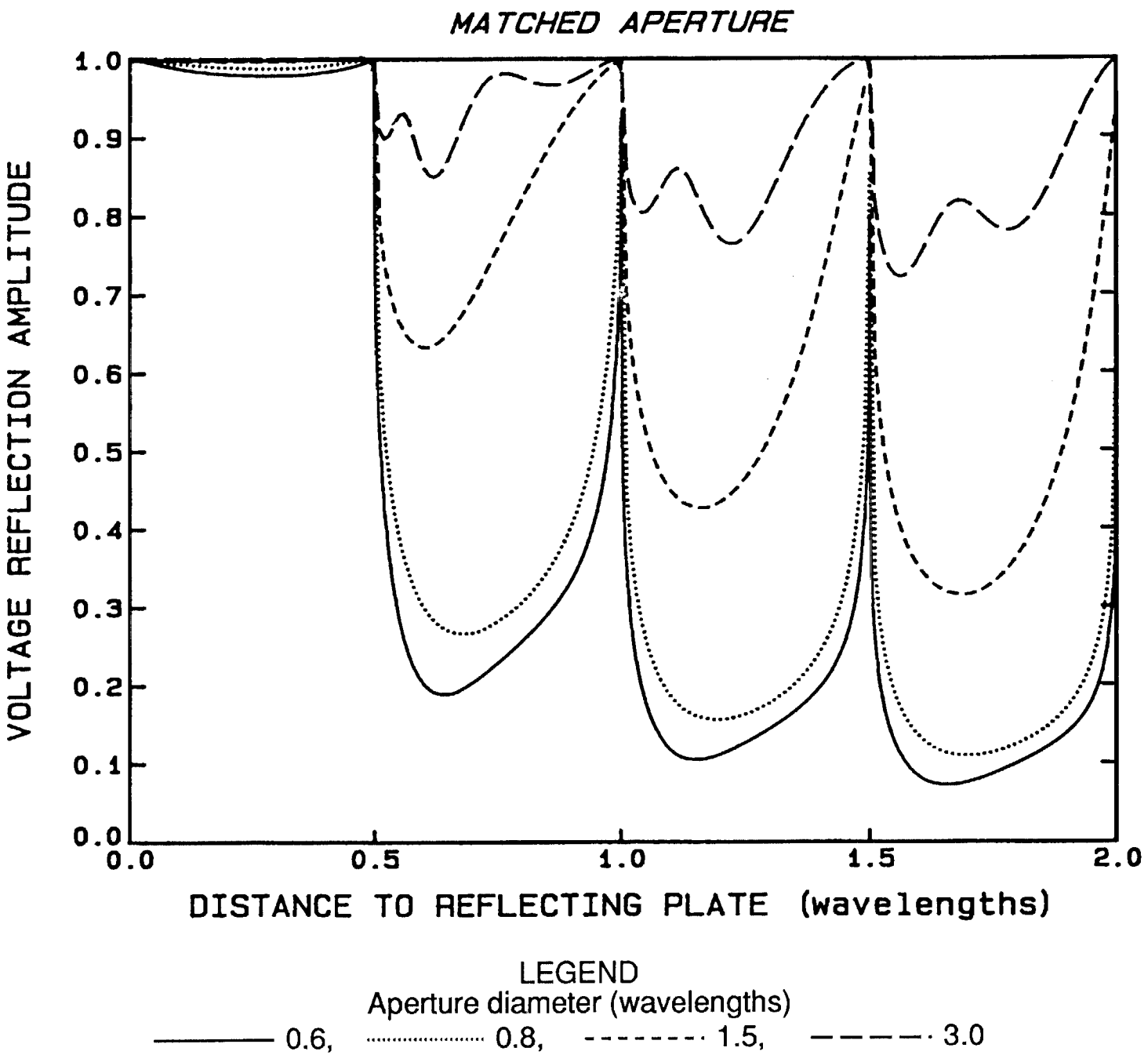

Figure 17.-Reflection coefficient magnitude vs. plate spacing.

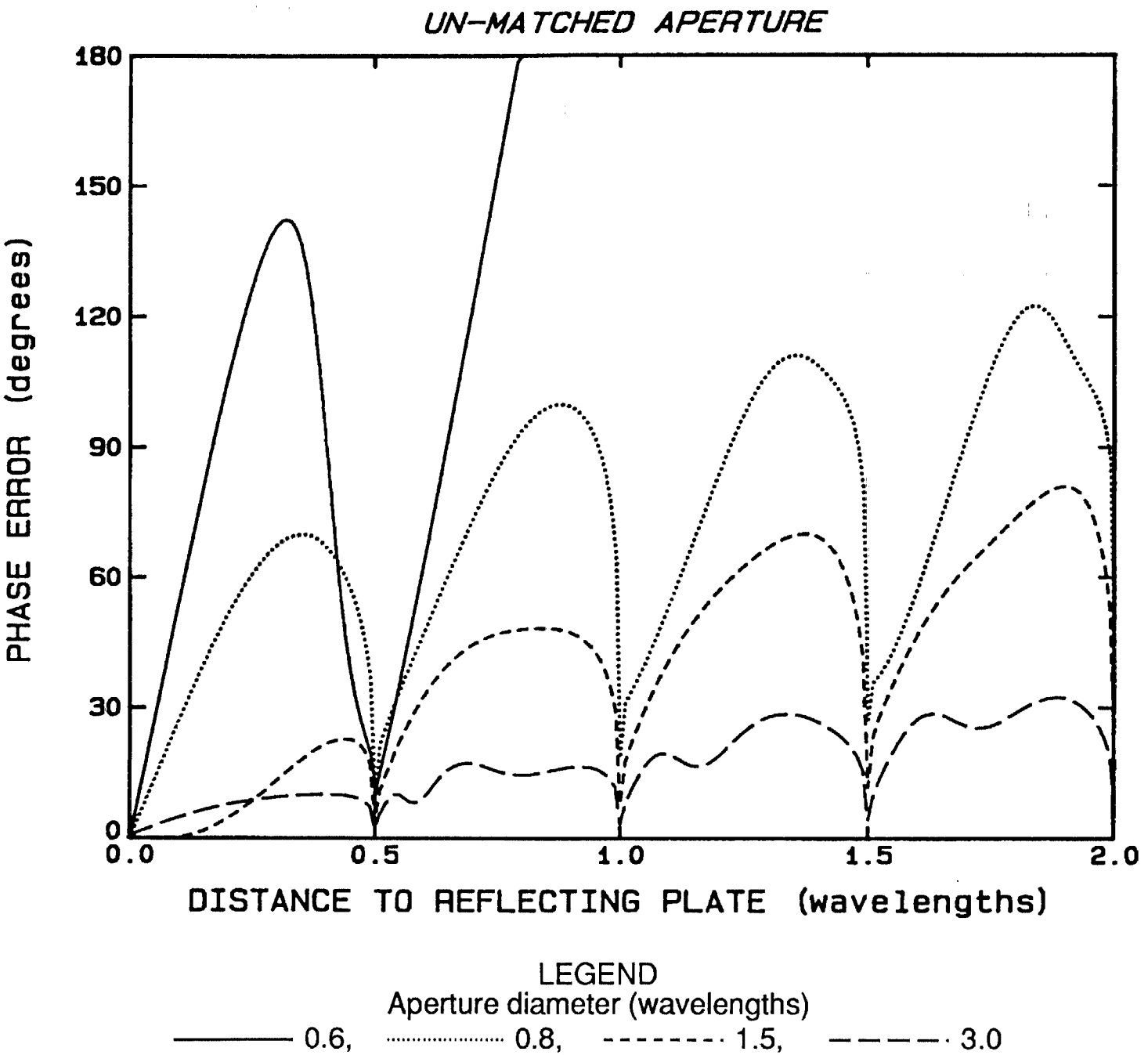

Figure 18.-Phase error vs. plate spacing.

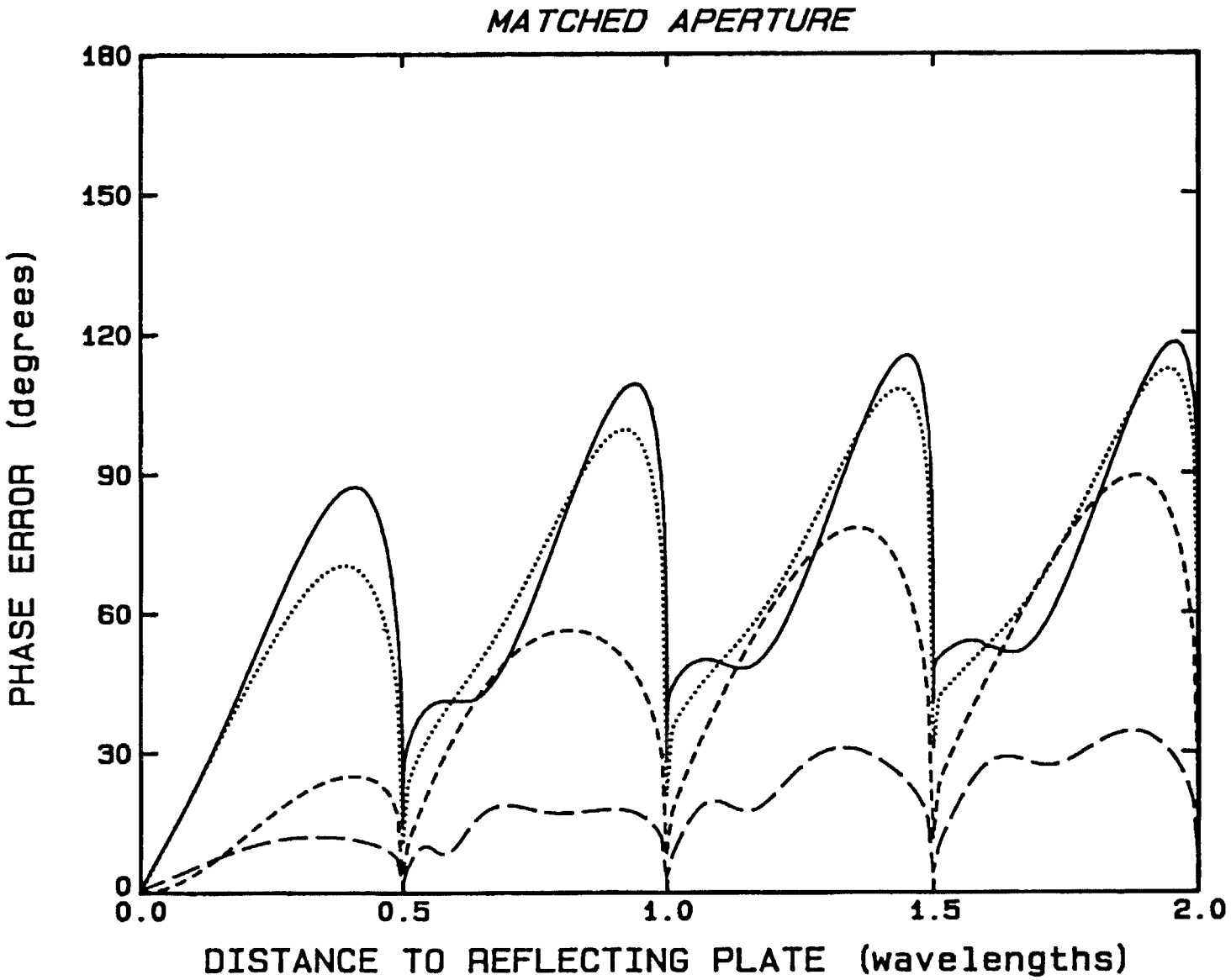

Figure 19.-Phase error vs. plate spacing.

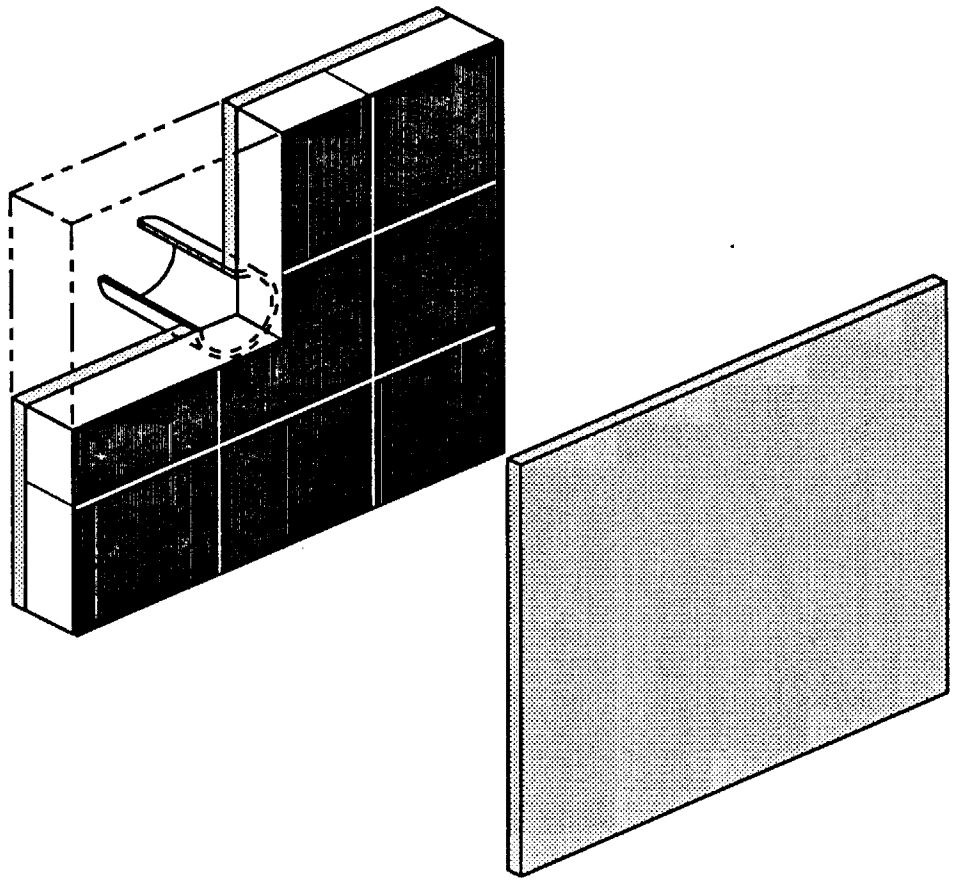

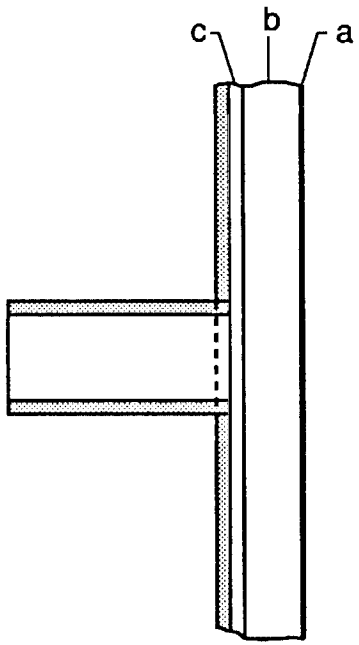

TILE MODEL PARAMETERS

Layer	ε_R	Thickness, in.
a	4.8 - j0.0144	0.015
b	1.2 - j0.00108	0.900
c	1.0 - j0.00001	0.177

Figure 20.-Physical and mathematical model of circular aperture with dielectric tile cover.

891317.011.024/A

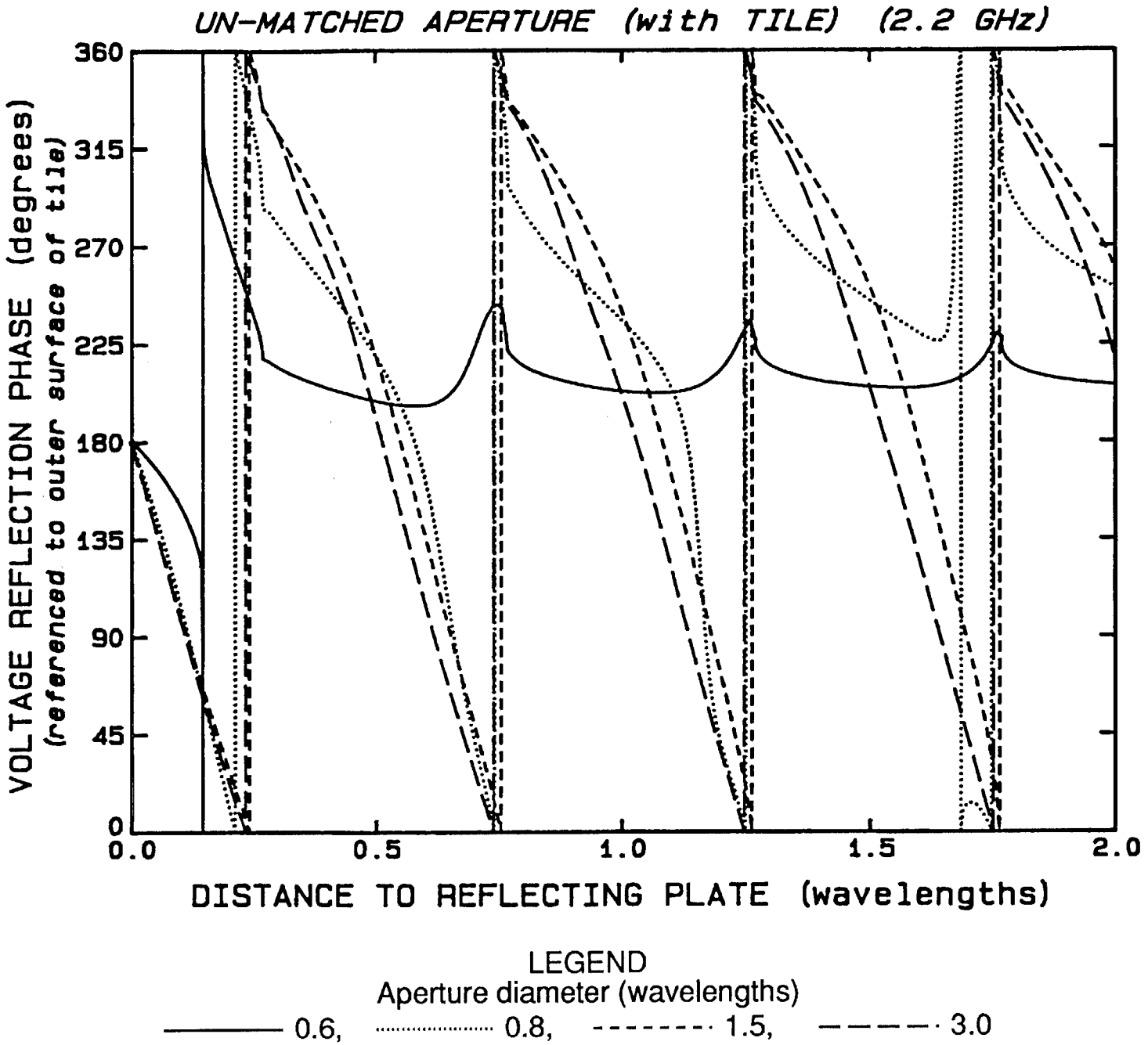

Figure 21.-Reflection coefficient phase vs. plate spacing.

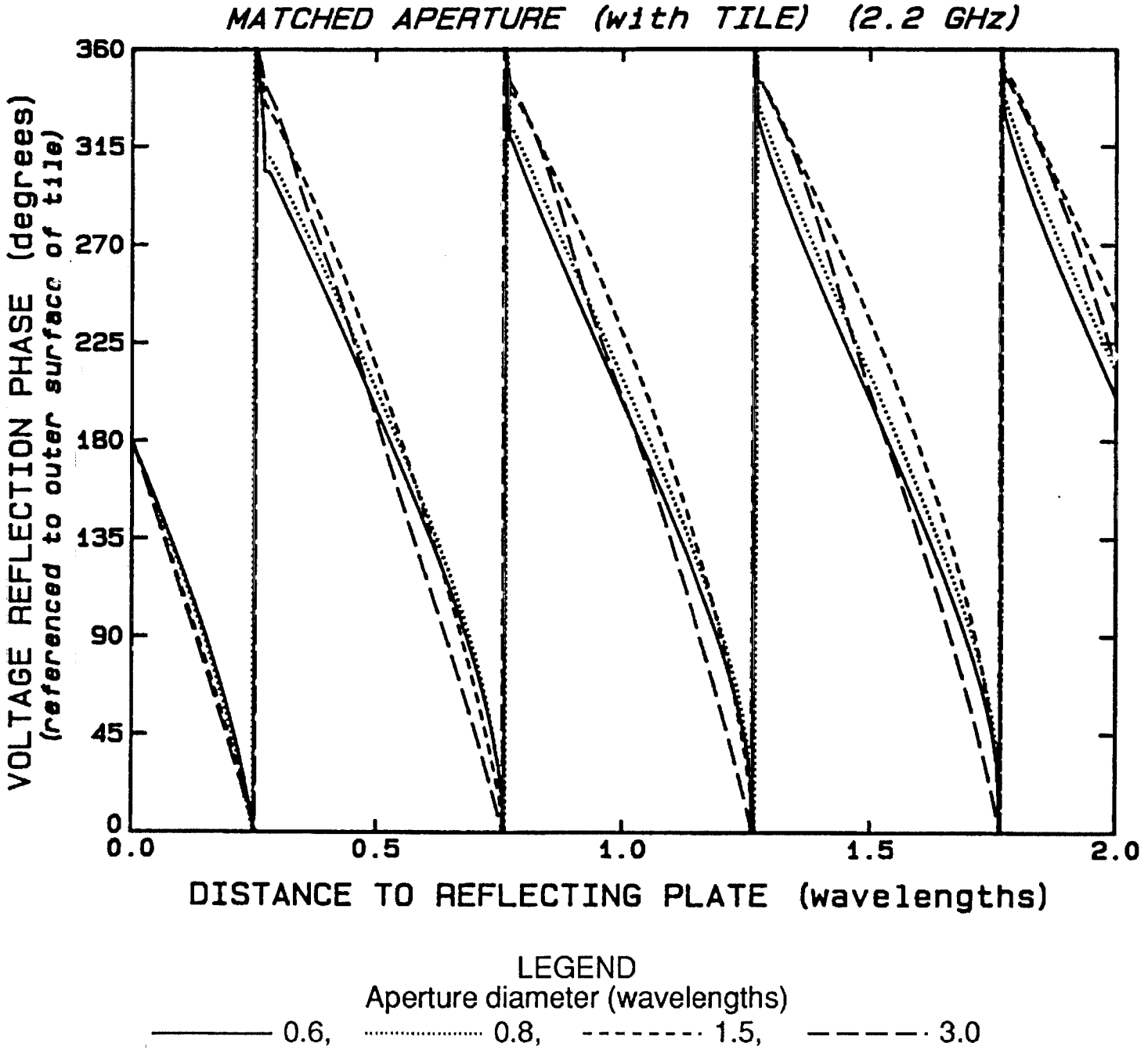

Figure 22.-Reflection coefficient phase vs. plate spacing.

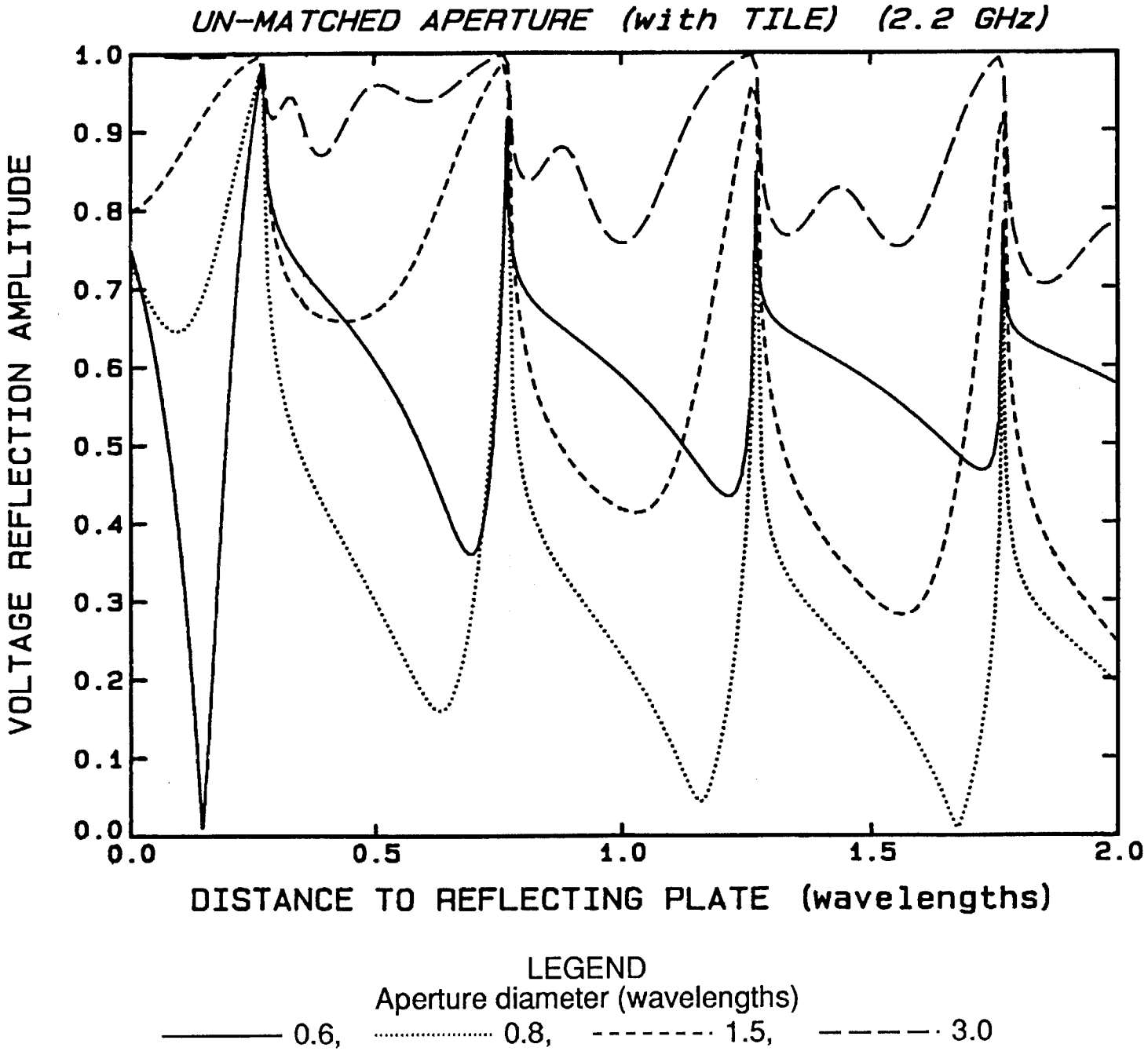

Figure 23.-Reflection coefficient magnitude vs. plate spacing.

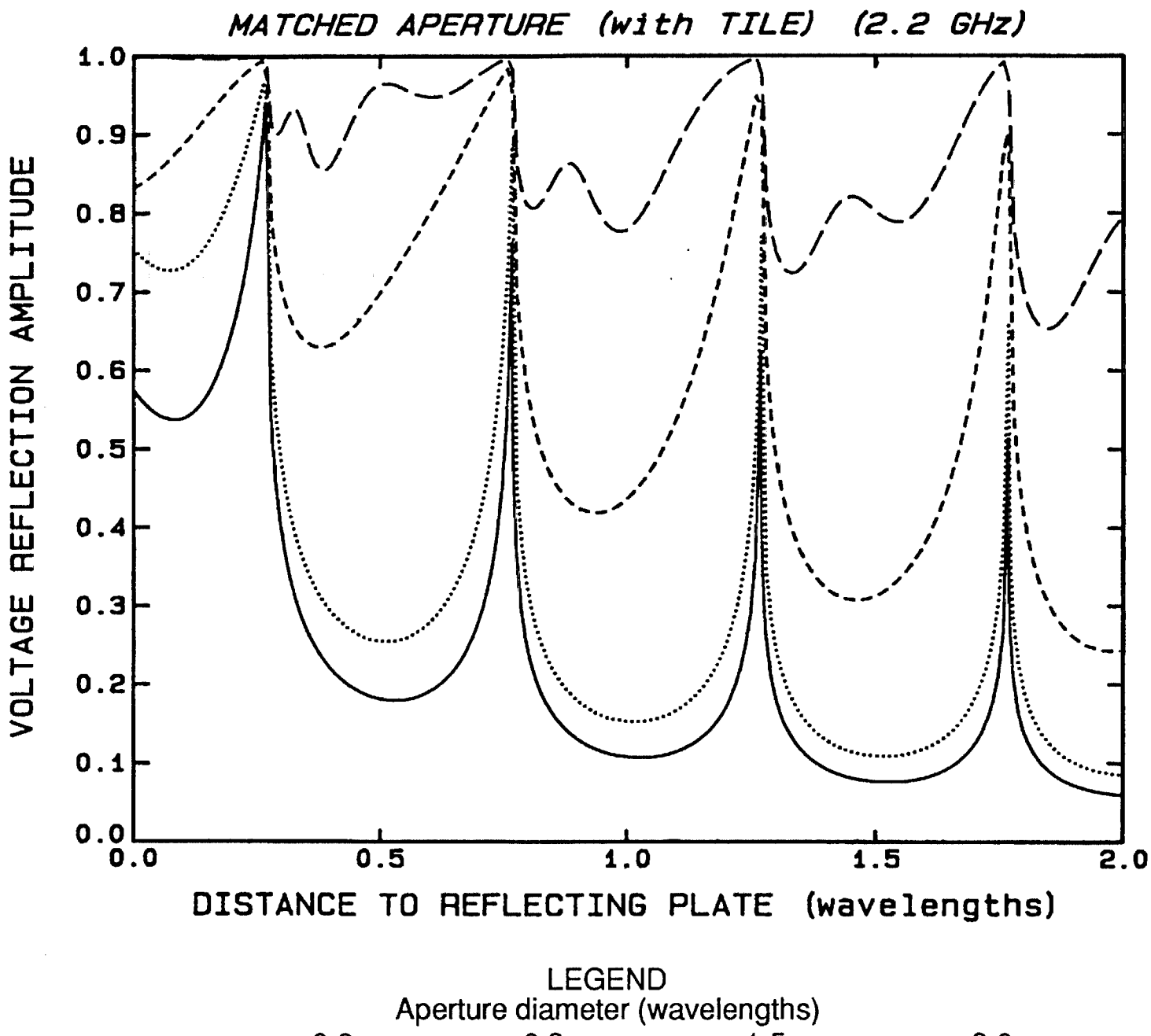

Figure 24.-Reflection coefficient magnitude vs. plate spacing.

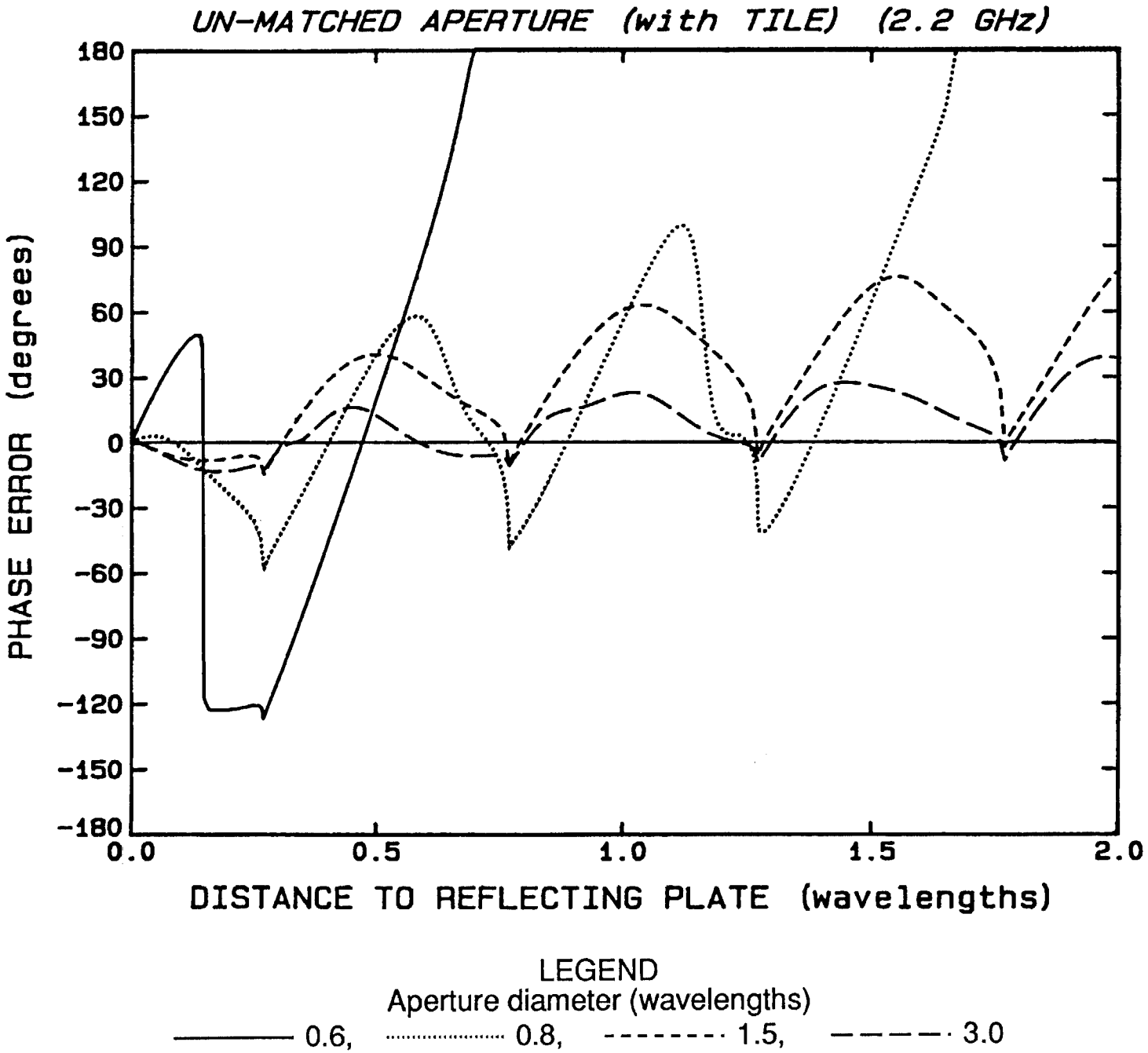

Figure 25.-Phase error vs. plate spacing.

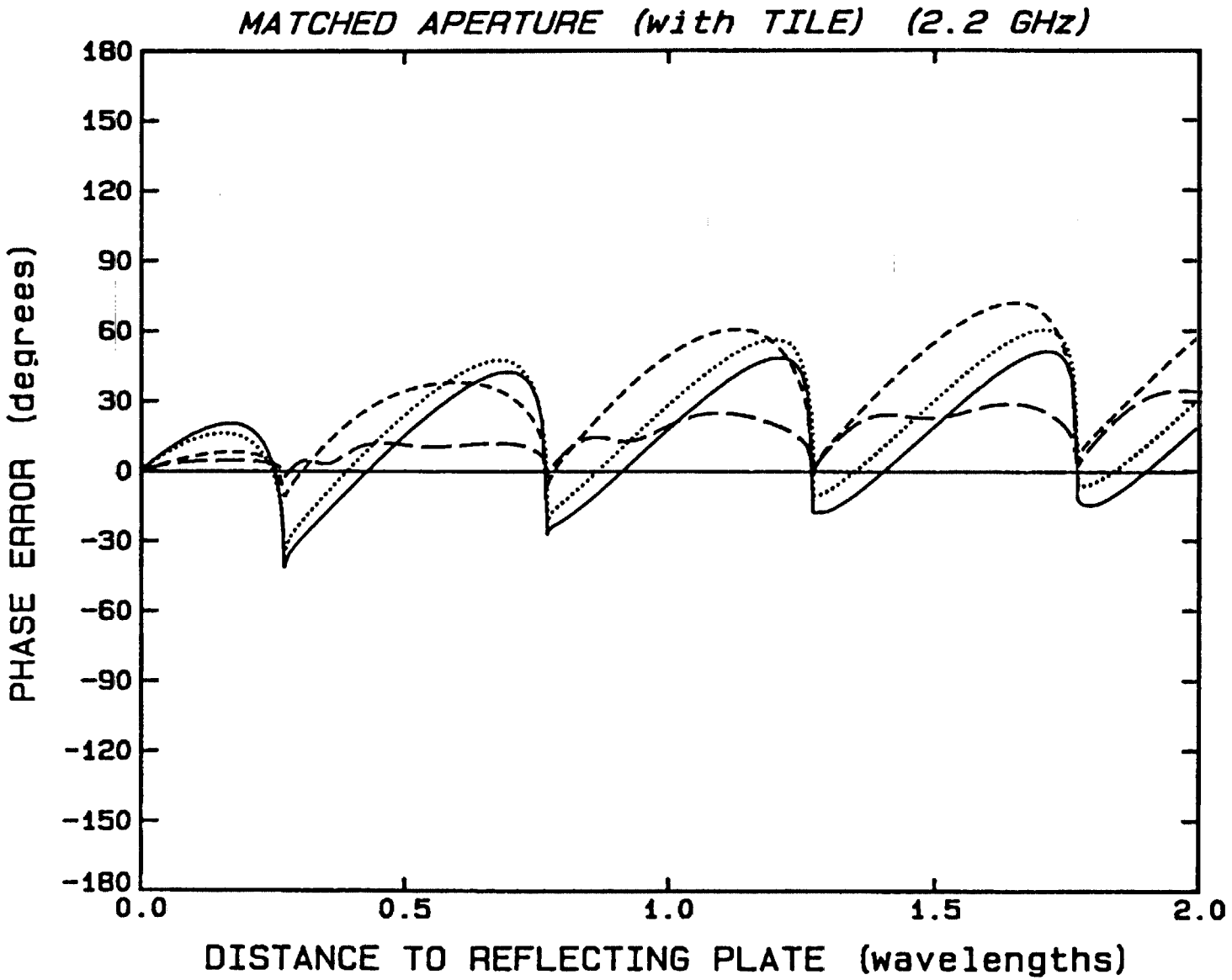

Figure 26.-Phase error vs. plate spacing.

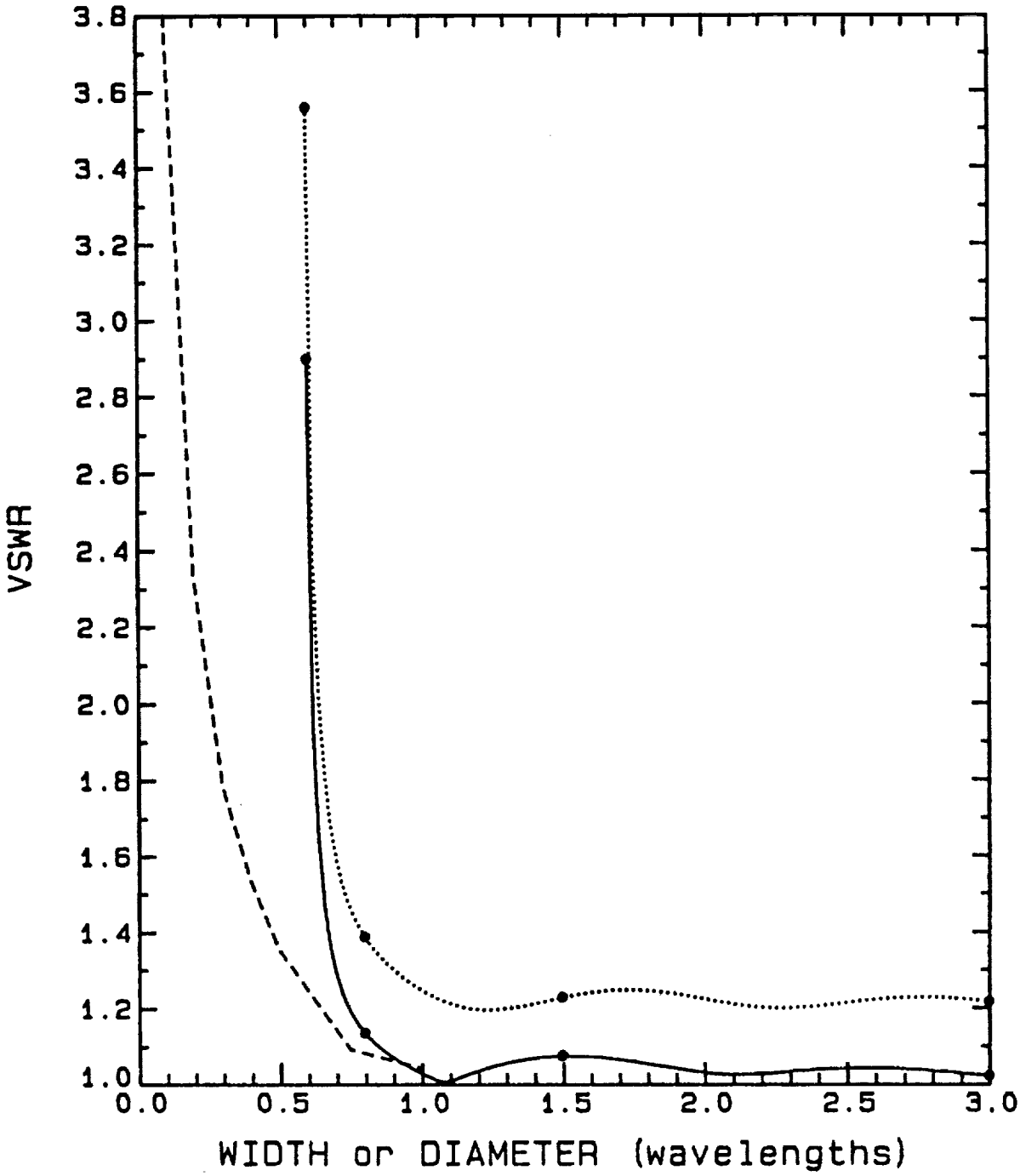

Figure 27.-Free-space VSWR vs. aperture size

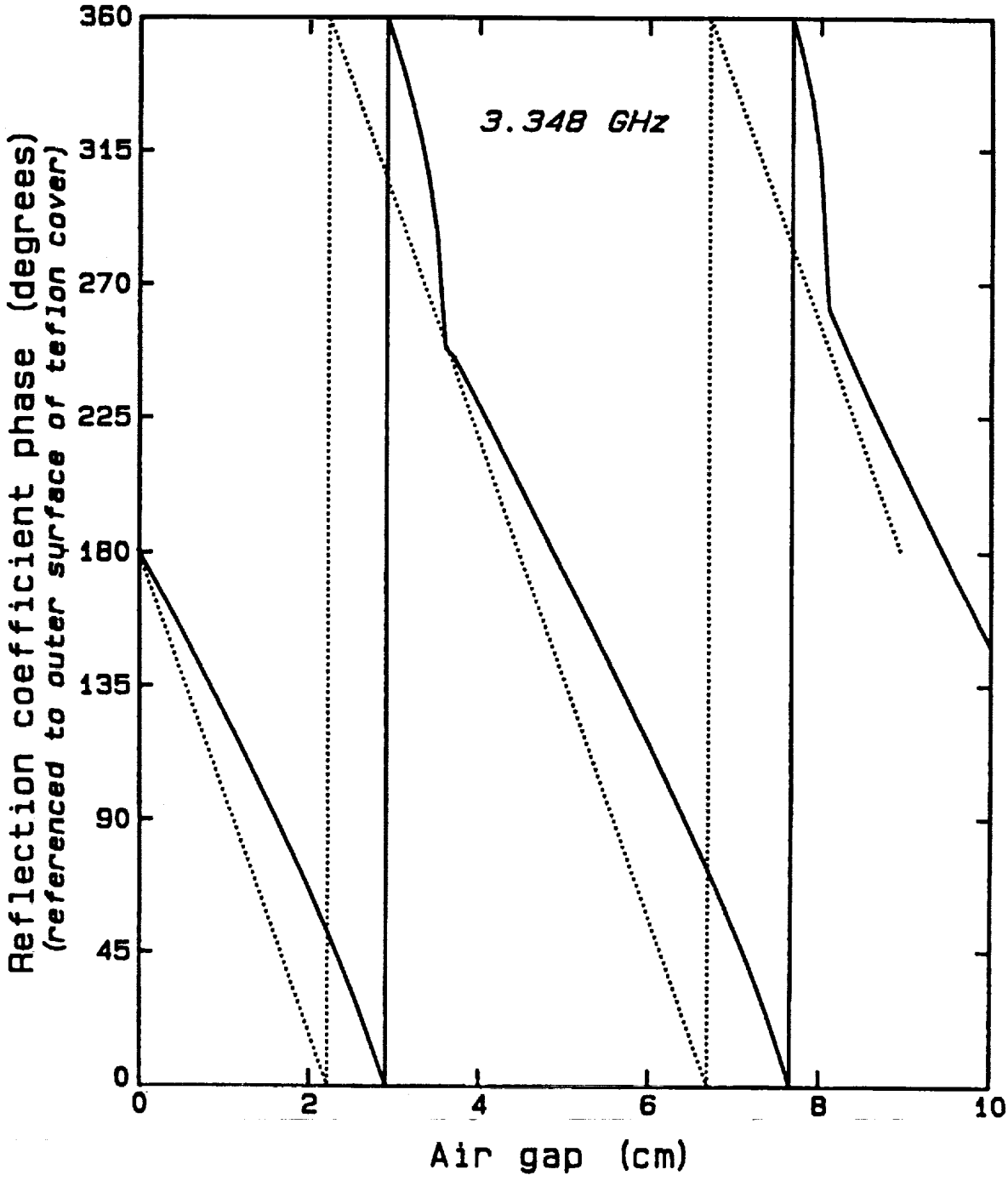

LEGEND

——— Calculated ····· Ideal

Figure 28.-Reflection coefficient phase for circular aperture with tile cover.

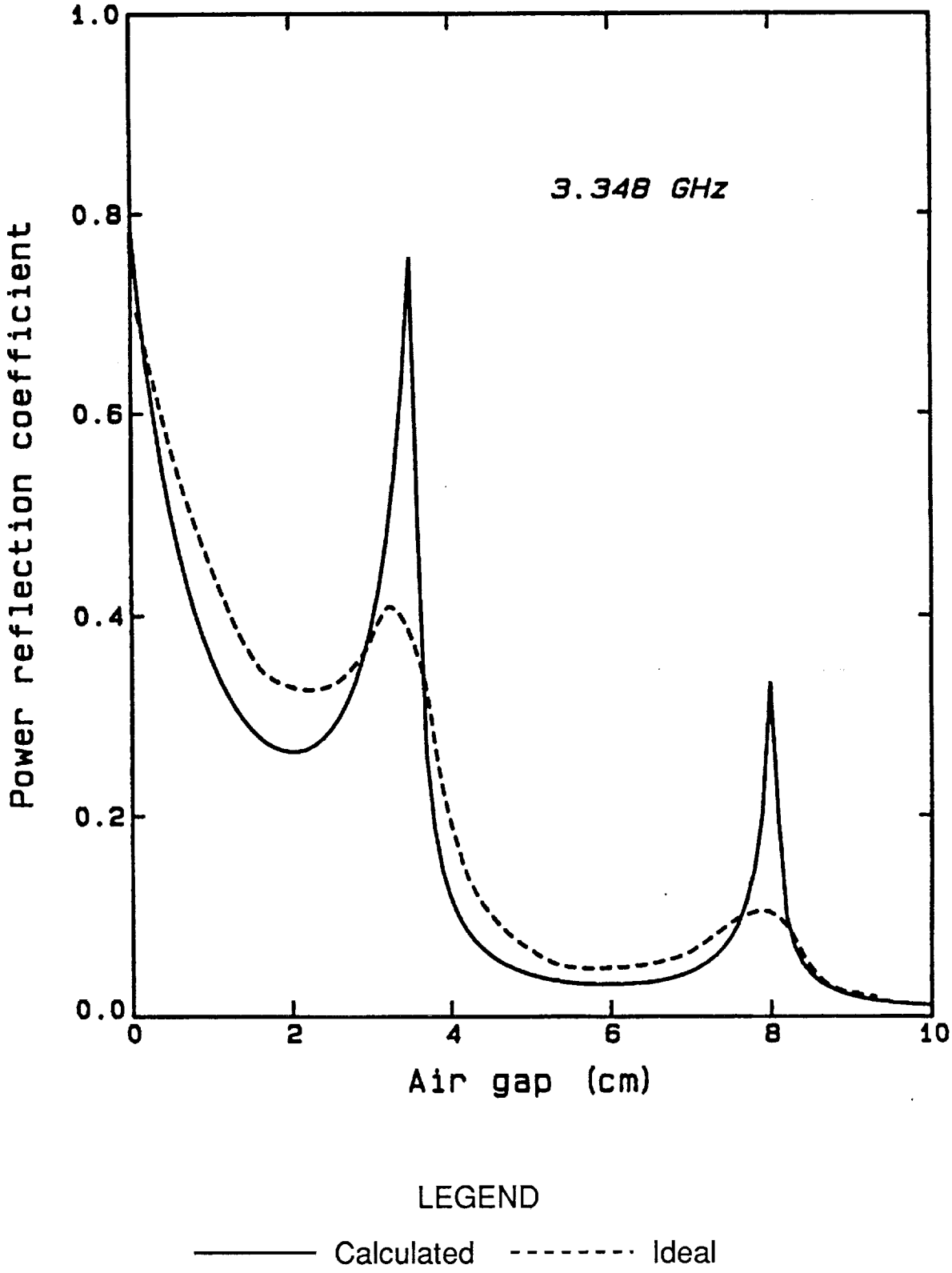

Figure 29.-Theoretical and measured power reflection coefficient for tile covered circular aperture.

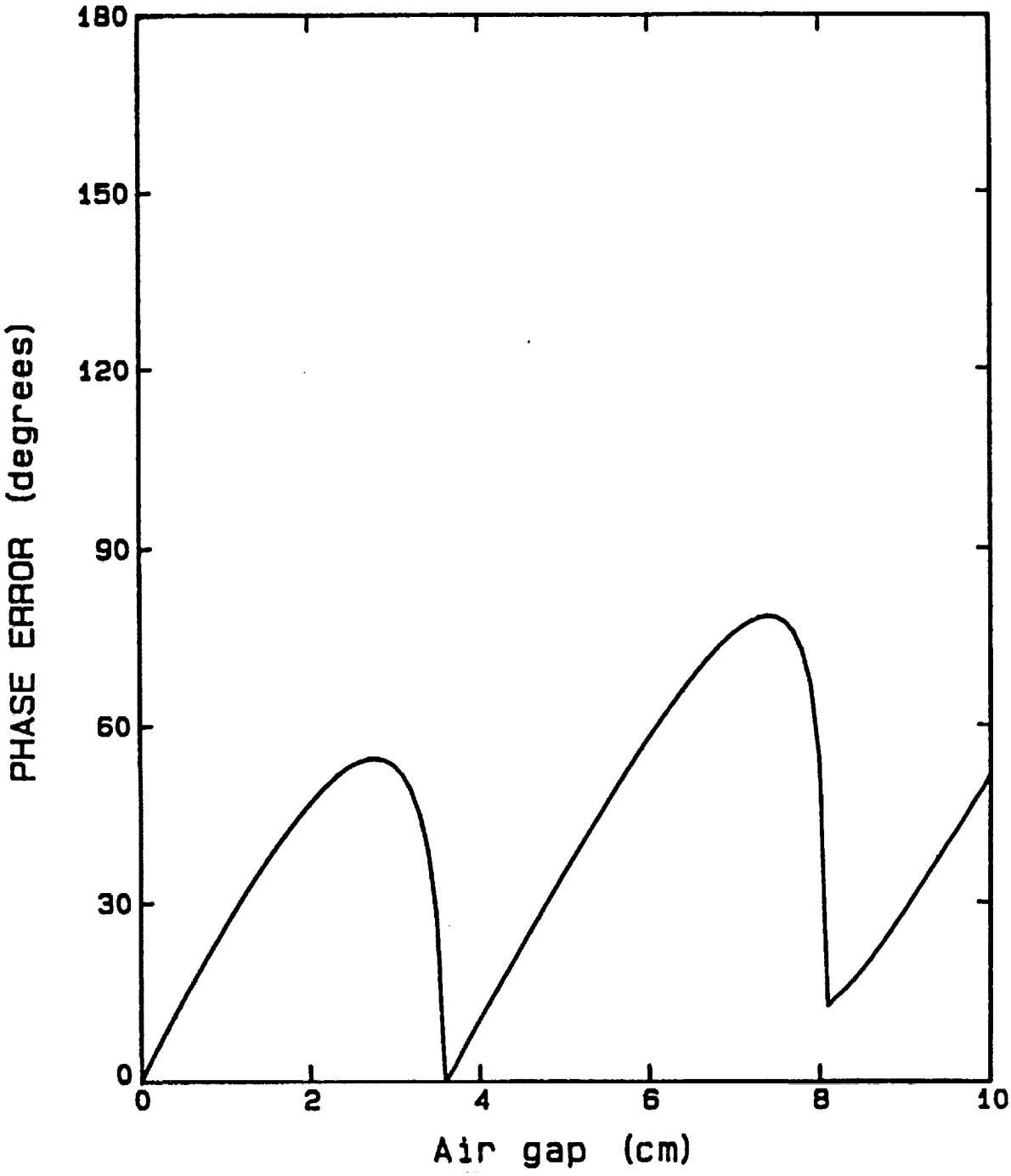

Figure 30.-Theoretical phase error for tile-covered aperture.

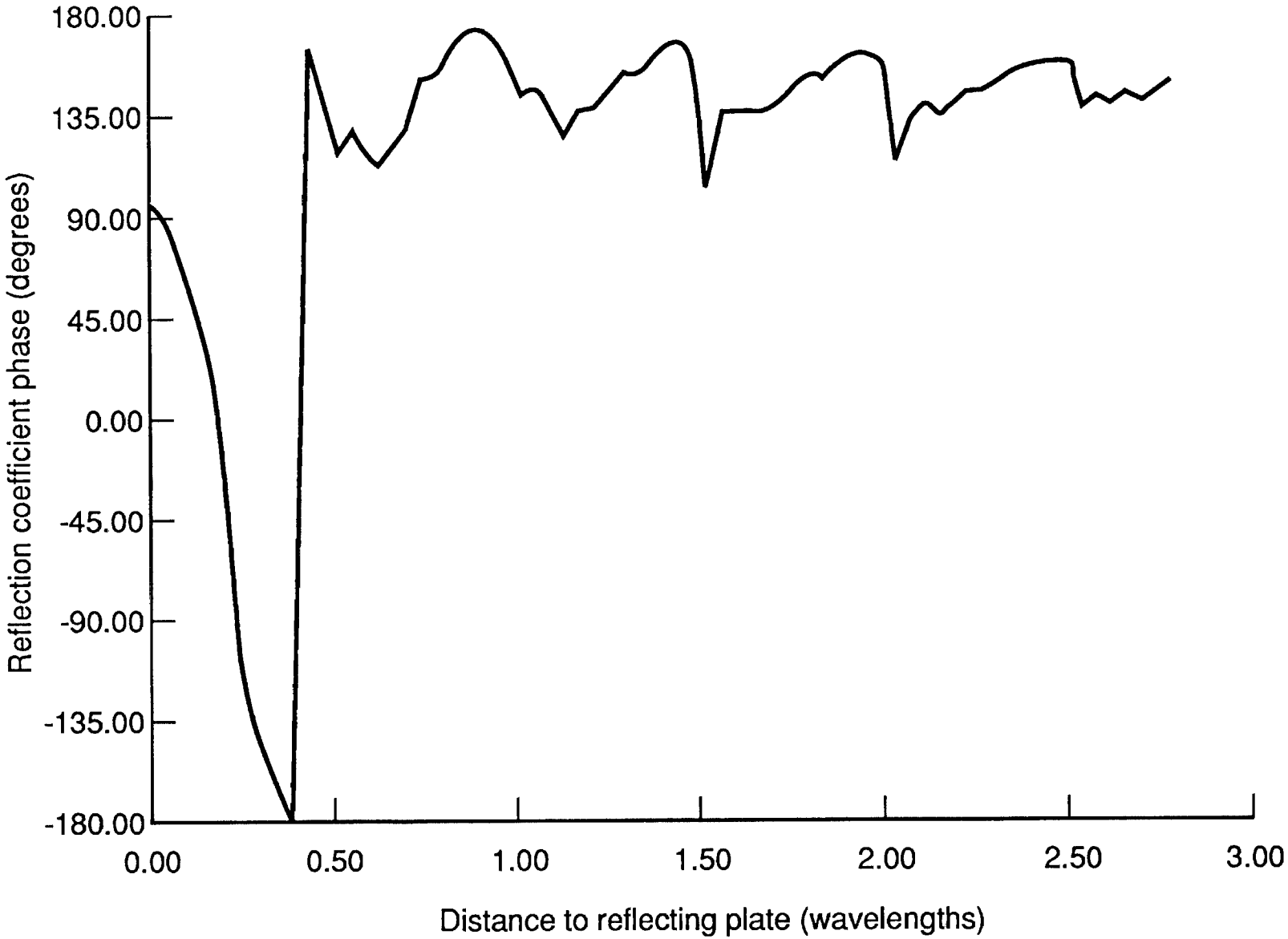

Figure 31.-Measured reflection coefficient phase vs. plate spacing.

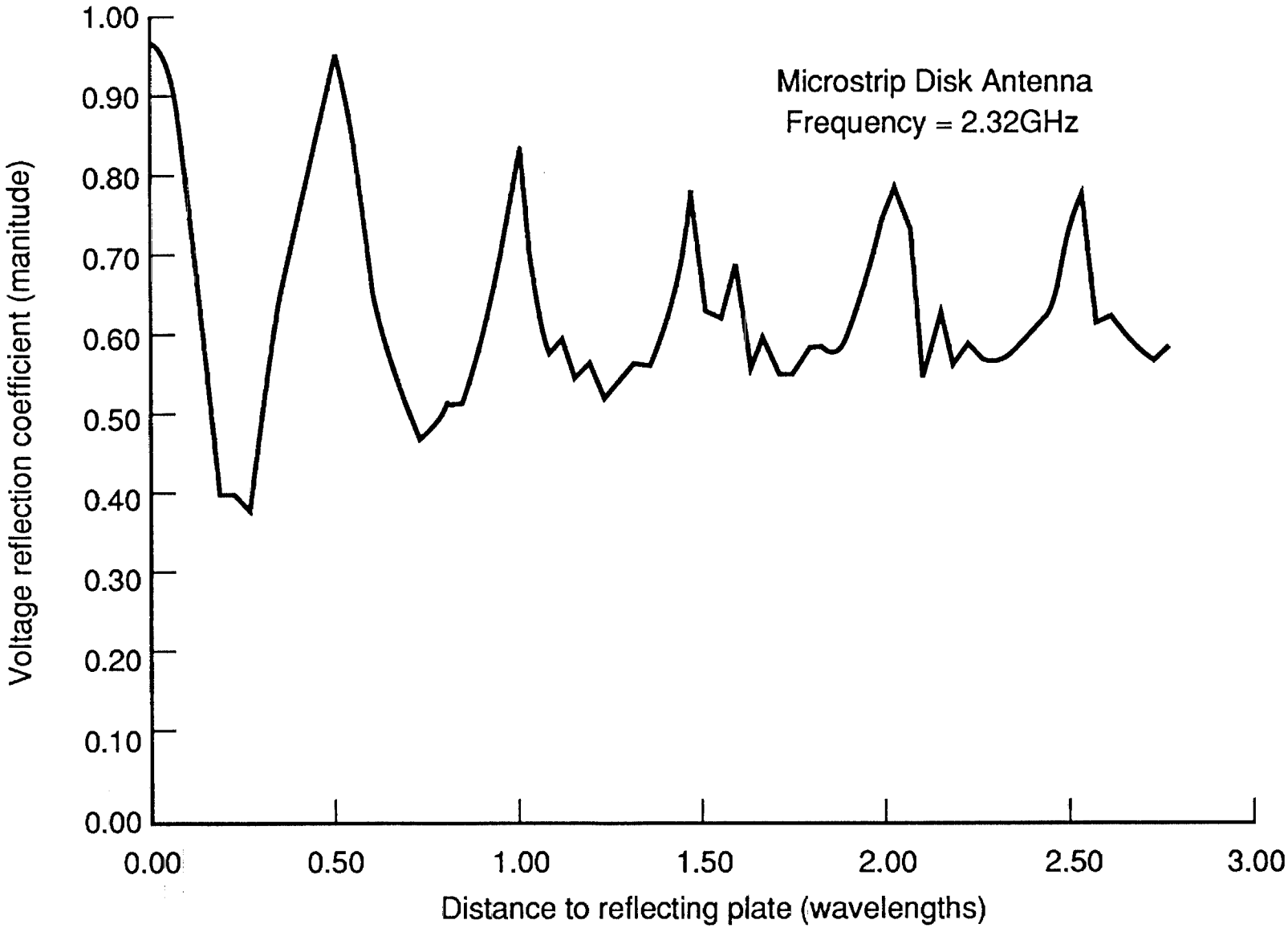

Figure 32.-Measured reflection coefficient vs. plate spacing.

NASA National Aeronautics and Space Administration

Report Documentation Page

1. Report No.	2. Government Accession No.	3. Recipient's Catalog No.
NASA TM-101680		

4. Title and Subtitle
An Assessment of the Potential of Continuous-Wave Ranging for Measuring the Distance to a Highly Reflective, Infinite Sheet

5. Report Date
April 1990

6. Performing Organization Code

7. Author(s)
C. P. Hearn
M. C. Bailey
M. J. Czerner
K. L. Dudley E. Vedeler

8. Performing Organization Report No.

10. Work Unit No.
506-44-21-03

9. Performing Organization Name and Address
NASA Langley Research Center
Hampton, VA 23665-5225

11. Contract or Grant No.

13. Type of Report and Period Covered
Technical Memorandum

12. Sponsoring Agency Name and Address
National Aeronautics and Space Administration
Washington, DC 20546-0001

14. Sponsoring Agency Code

15. Supplementary Notes

16. Abstract
This paper examines the feasibility of a continuous-wave, distance-measuring technique for measuring the distance from a spacecraft antenna to a highly ionized plasma surface. The reflection coefficient angle is computed for several aperture models. It is concluded that aperture size and the presence of a nonablating dielectric cover over the antenna are critical factors.

17. Key Words (Suggested by Author(s))	18. Distribution Statement
distance measurement plasma diagnostics	unclassified - unlimited subject category 33

19. Security Classif. (of this report)	20. Security Classif. (of this page)	21. No. of pages	22. Price
unclassified	unclassified	49	A03